Annual Methodological Archive Research Review
http://amresearchreview.com/index.php/Journal/about
Volume 4, Issue 6 (2026)

Online ISSN 3007-3197
Print ISSN 3007-3189

http://amresearchreview.com/index.php/Journal/about

In Silico Design, Molecular Docking, Molecular Dynamics Simulation, and ADMET Evaluation of Novel Quinazoline Derivatives as EGFR Inhibitors for Non-Small-Cell Lung Cancer

Marwa Zulfiqar Ali

Faculty of Biological Sciences, Superior University, Lahore. marwahzulfiqar65@gmail.com

Dr. Rashid Mahmood

Assistant Professor, Faculty of Biological Sciences, Superior University, Lahore. rashidqcm@gmail.com

ABSTRACT

Lung cancer continues to be one of the biggest killers of cancer patients in the world, and constant development of safer and effective targeted therapies is still required. In this study, the rational design and computational assessment of novel quinazoline-based ligands as inhibitors of the epidermal growth factor receptor (EGFR), which is an important therapeutic target in non-small-cell lung cancer (NSCLC), is investigated. Ten novel quinazoline derivatives (QZ-01 to QZ-10) were designed by structurally modifying the 4-anilinoquinazoline scaffold. To identify binding affinities and poses, 100 ns molecular dynamics (MD) simulations were performed with GROMACS on the top docked complexes, and molecular docking was carried out with AutoDock Vina. Root Mean Square Deviation (RMSD), Root Mean Square Fluctuation (RMSF), radius of gyration (Rg), hydrogen-bond occupancy, and MM-GBSA binding free-energy calculations were used to comprehensively evaluate the stability of the complexes. Besides, SwissADME and pkCSM were used for drug-likeness prediction and pharmacokinetic (ADMET) properties prediction. The docking score from the results shows that the three compounds (QZ-08, QZ-07, and QZ-04) had a score of −9.82, −9.68, and −9.56 kcal/mol respectively, better than the reference drug erlotinib with a score of −8.73 kcal/mol. QZ-08 had the lowest average RMSD and RMSF of 1.82 Å and 0.74 Å respectively, and hydrogen-bond occupancy of 93.2% along with MM-GBSA binding energy of −63.15 kcal/mol compared to those of erlotinib as −48.73 kcal/mol during

Annual Methodological Archive Research Review
http://amresearchreview.com/index.php/Journal/about
Volume 4, Issue 6 (2026)

Online ISSN 3007-3197
Print ISSN 3007-3189
http://amresearchreview.com/index.php/Journal/about

MD simulations. QZ-07 also showed strong structural stability and good binding affinity to key residues in EGFR such as Met793, Lys745, Asp855, and Cys797. Both candidates were calculated to have high gastrointestinal absorption and strict compliance with Lipinski's Rule of Five (RO5) with no AMES mutagenicity and minor cardiotoxicity. This computational workflow was integrated and allowed the evaluation of binding strength, conformational stability, pharmacokinetic suitability and safety simultaneously. Finally, QZ-08 and QZ-07 are extremely promising computational leads that are suggested for further synthesis and biological evaluation as possible EGFR targeted anticancer agents.

Keywords: Quinazoline Derivatives; Epidermal Growth Factor Receptor (EGFR); Non-Small-Cell Lung Cancer (NSCLC); Molecular Docking; Molecular Dynamics Simulation.

1. Introduction

Cancer is one of the major causes of death globally and is one of the most urgent public health problems of today. It is a complicated group of conditions that involves growth of cells that are not controlled, invasion of nearby tissues, and metastasis [1]. Prevalent risk factors are expected to lead to a significant growth in the burden of cancer in the next few decades. According to estimates, 20 million people were diagnosed with cancer and 9.7 million cancer deaths occurred worldwide in 2022. Among these new cases were 2.5 million cases of lung cancer (12.4%) which accounted for the highest cancer-related mortality (18.7%) [1].

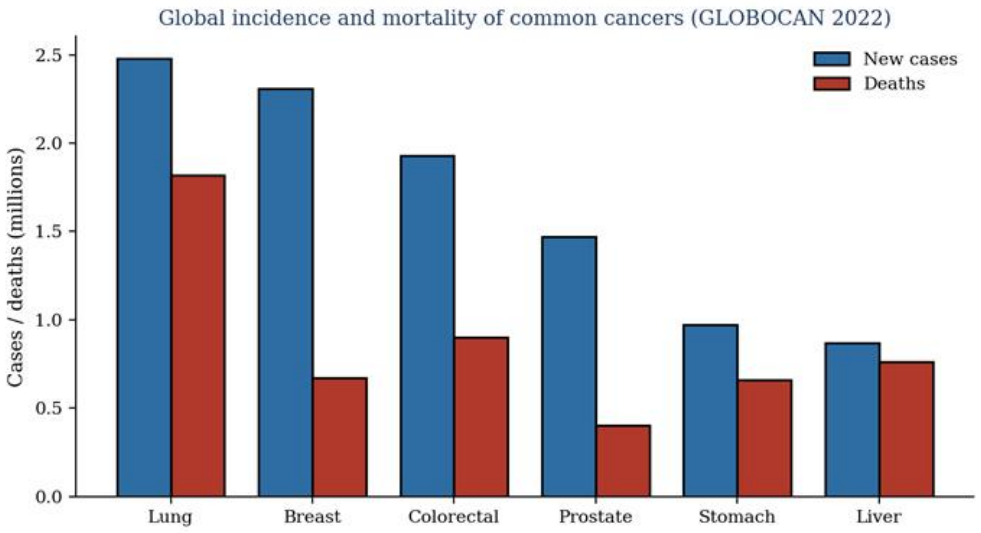

Figure 1.1: Estimated global incidence and mortality of the most common cancers

Annual Methodological Archive Research Review
http://amresearchreview.com/index.php/Journal/about
Volume 4, Issue 6 (2026)

Online ISSN 3007-3197
Print ISSN 3007-3189
http://amresearchreview.com/index.php/Journal/about

worldwide, highlighting the burden of lung cancer (data from GLOBOCAN 2022). Lung cancer has a high mortality rate due to late diagnosis, aggressive disease and metastasis. Traditional treatment such as surgery, radiation and cytotoxic chemotherapy slows the growth of rapidly growing cells, but are nonselective and therefore have unwanted side effects and can cause resistance [2, 5, 6]. However, targeted treatments focus drugs on specific molecular targets that are crucial for tumour growth, offering more therapeutic benefits without the side effects [4].

Non-small-cell lung cancer (NSCLC) makes up approximately 85% of all cases of lung cancer, including adenocarcinoma, squamous-cell carcinoma, and large-cell carcinoma. Although modifiable risk factors (such as tobacco use) play a role in the disease, certain oncogenic mutations that stimulate growth-promoting pathways have a significant role, particularly in non-smokers. One of the major molecular events in NSCLC is the epidermal growth factor receptor (EGFR) [7].

EGFR, a receptor tyrosine kinase involved in cell proliferation, differentiation and cell survival. It is composed of an extracellular, ligand binding domain, a transmembrane helix, an intracellular tyrosine-kinase domain, and a C-terminal regulatory tail [7].

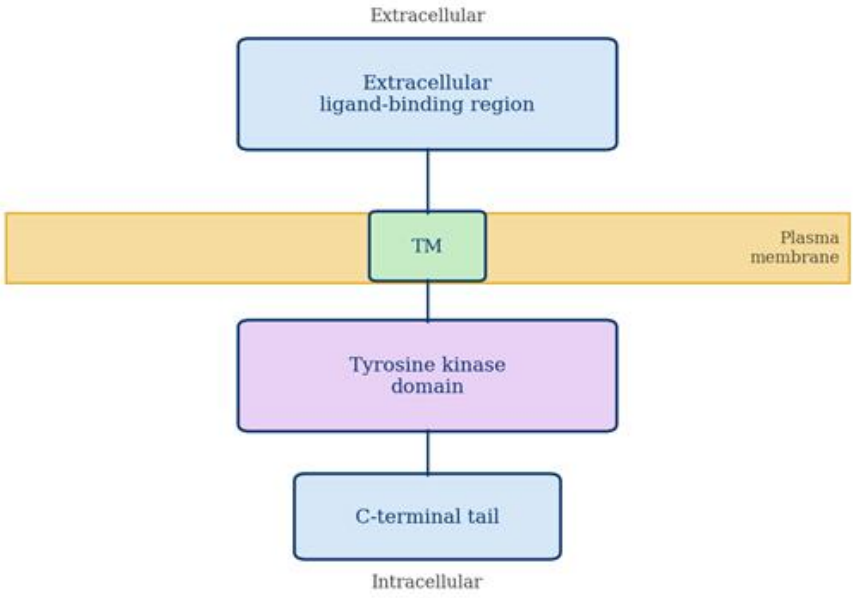

Figure 1.2: Schematic representation of the domain architecture of the epidermal growth factor receptor (EGFR).

Annual Methodological Archive Research Review
http://amresearchreview.com/index.php/Journal/about
Volume 4, Issue 6 (2026)

Online ISSN 3007-3197
Print ISSN 3007-3189
http://amresearchreview.com/index.php/Journal/about

EGFR binding to a ligand result in dimerization and autophosphorylation of the receptor, thereby activating downstream pathways like the RAS-RAF-MEK-ERK pathway, PI3K-AKT-mTOR pathway, and JAK-STAT pathway, all of which contribute to cell proliferation, survival, and migration [4].

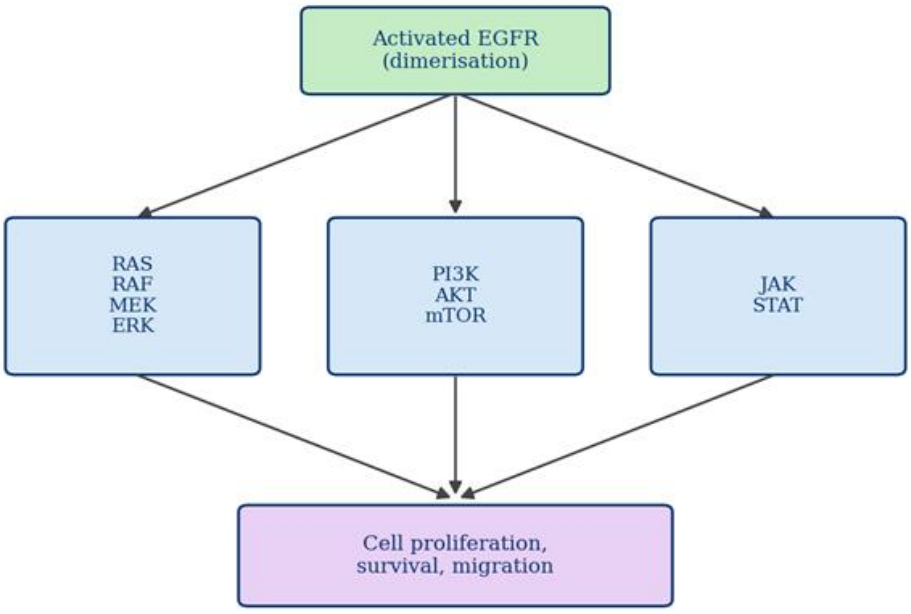

Figure 1.3: Major downstream signalling pathways activated by EGFR that regulate cell proliferation, survival, and migration.

Activating mutations in the tyrosine-kinase domain, as the most common, are the exon-19 deletions and exon-21 L858R mutation of EGFR, which is often associated with constitutive activation in NSCLC. These mutations cause a shift in the inactive kinase conformation to make it more favorable to bind ATP-competitive inhibitors. In turn, the development of first generation (gefitinib and erlotinib) and second generation (afatinib) irreversible inhibitors has been the result of these attempts to target the mutant forms [8].

Annual Methodological Archive Research Review
http://amresearchreview.com/index.php/Journal/about
Volume 4, Issue 6 (2026)

Online ISSN 3007-3197
Print ISSN 3007-3189
http://amresearchreview.com/index.php/Journal/about

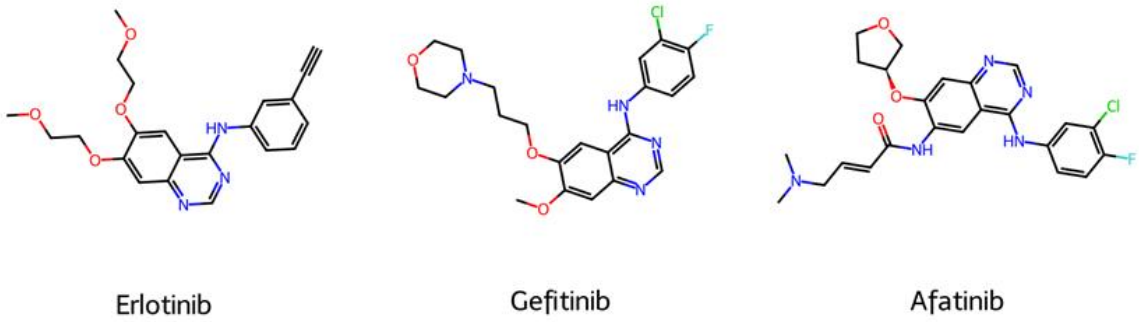

Figure 1.4: Chemical structures of representative clinically approved quinazoline-based EGFR tyrosine-kinase inhibitors.

Table 2.1: ***Successive generations of EGFR tyrosine-kinase inhibitors, showing representative agents, binding mode, principal activity, and the resistance that limits each generation (compiled from [4] and [9]).***

Generation	Representative agents	Binding mode	Principal activity / target	Key limitation / resistance
First	Gefitinib, erlotinib	Reversible, ATP-competitive	Activating mutations (exon-19 deletion, L858R) and wild-type EGFR	Resistance through the T790M gatekeeper mutation
Second	Afatinib, dacomitinib	Irreversible, covalent (pan-ErbB)	Activating mutations; broader ErbB-family inhibition	Limited anti-T790M activity at tolerable doses; wild-type toxicity
Third	Osimertinib	Irreversible, mutant-selective	T790M together with activating	Resistance through the C797S mutation and bypass

Annual Methodological Archive Research Review
http://amresearchreview.com/index.php/Journal/about
Volume 4, Issue 6 (2026)

Online ISSN 3007-3197
Print ISSN 3007-3189
http://amresearchreview.com/index.php/Journal/about

Generation	Representative agents	Binding mode	Principal activity / target	Key limitation / resistance
			mutations; spares wild-type	pathways
Fourth (emerging)	Allosteric inhibitors (in development)	Allosteric, non-ATP-competitive	C797S-containing triple-mutant EGFR	Still investigational; clinical efficacy being established

Acquired resistance is a major therapeutic challenge, yet can be seen in some remarkable clinical cases. The T790M gatekeeper mutation is a methionine for threonine substitution that can sterically obstruct binding of the inhibitors and reduces the affinity of both 1st and 2nd generation [8, 9]. Third generation inhibitors, such as osimertinib, have been developed that specifically target T790M containing receptors, but resistance has been observed through a mutation in the receptor, C797S, in which the cysteine residue necessary for covalent binding is removed [4, 9, 20]. The quinazoline nucleus has been known to have some resistance factors and recognized as a privileged scaffold in medicinal chemistry [10]. The quinazoline core, which is a fused benzene and pyrimidine ring structure, is the basis for erlotinib, gefitinib and afatinib [11, 17].

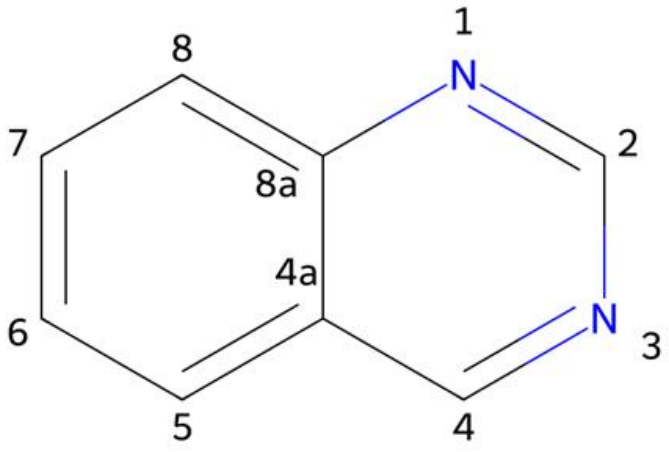

Figure 1.5: The core quinazoline scaffold showing conventional ring numbering and the key positions exploited in structural modification.

Annual Methodological Archive Research Review
http://amresearchreview.com/index.php/Journal/about
Volume 4, Issue 6 (2026)

Online ISSN 3007-3197
Print ISSN 3007-3189
http://amresearchreview.com/index.php/Journal/about

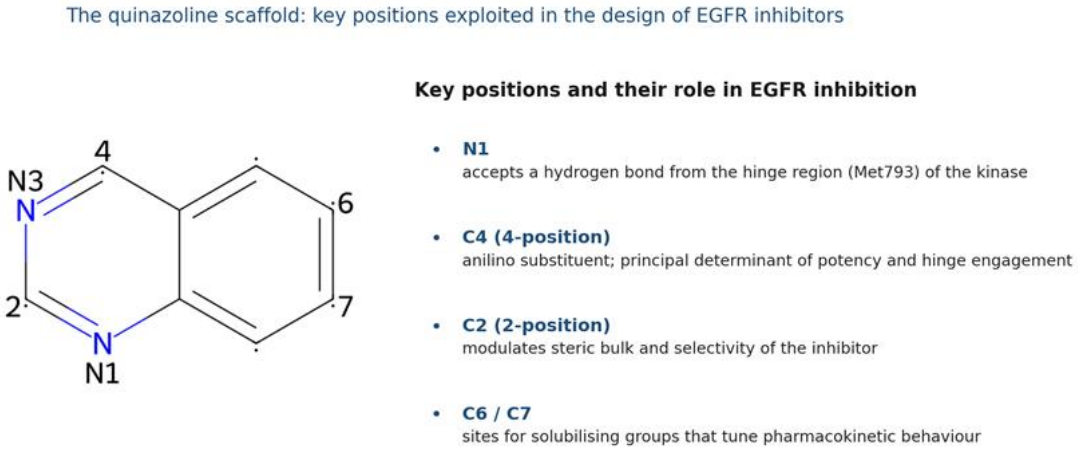

Figure 2.1: Key positions on the quinazoline scaffold exploited in the design of EGFR inhibitors and their principal roles in binding and pharmacokinetic optimization.

The N1 nitrogen of the quinazoline ring is involved in the important hydrogen bonding with the backbone NH of Met793 in the EGFR hinge region [12]. The main determinant of potency is the 4-anilino group, which fits well into the ATP site hydrophobic back pocket. Moreover, the 6- and 7-positions are in the solvent-exposed portion of the ATP cleft that can be modified to alter aqueous solubility and pharmacokinetic characteristics without greatly affecting intrinsic affinity [11].

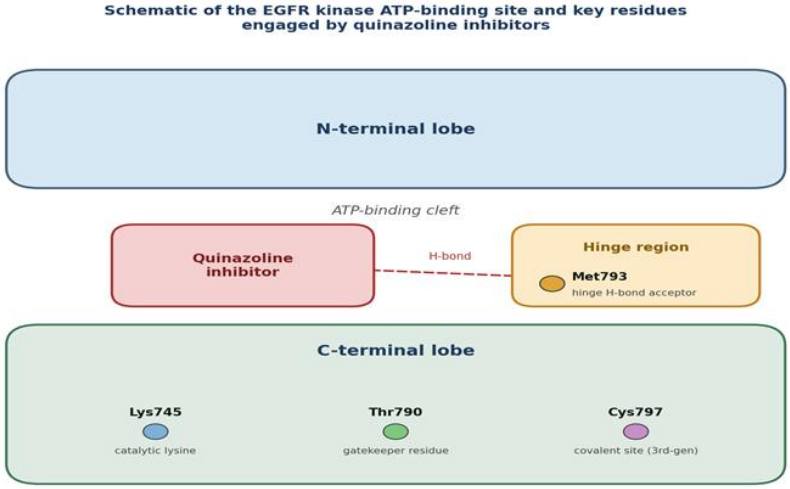

Figure 2.2: Schematic representation of the EGFR kinase ATP-binding site, showing the key residues (Met793, Thr790, Lys745, and Cys797) engaged by quinazoline-based inhibitors.

Annual Methodological Archive Research Review
http://amresearchreview.com/index.php/Journal/about
Volume 4, Issue 6 (2026)

Online ISSN 3007-3197
Print ISSN 3007-3189
http://amresearchreview.com/index.php/Journal/about

Therefore, new quinazoline derivatives with improved binding properties and PK could be designed to overcome the dynamic mutational nature of EGFR. This can be achieved with a streamlined cost-effective process by Computer-Aided Drug Design (CADD) [13, 14].

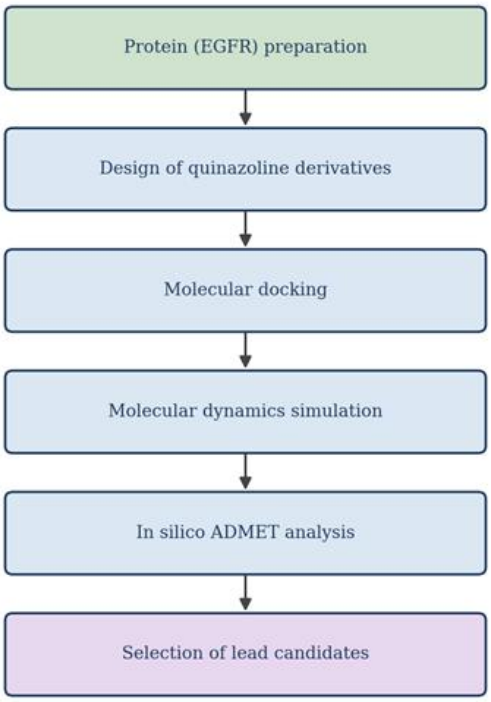

Figure 1.6: General computer-aided drug-design workflow adopted in the present study, combining molecular docking, molecular dynamics simulation, and in silico ADMET analysis.

Annual Methodological Archive Research Review
http://amresearchreview.com/index.php/Journal/about
Volume 4, Issue 6 (2026)

Online ISSN 3007-3197
Print ISSN 3007-3189
http://amresearchreview.com/index.php/Journal/about

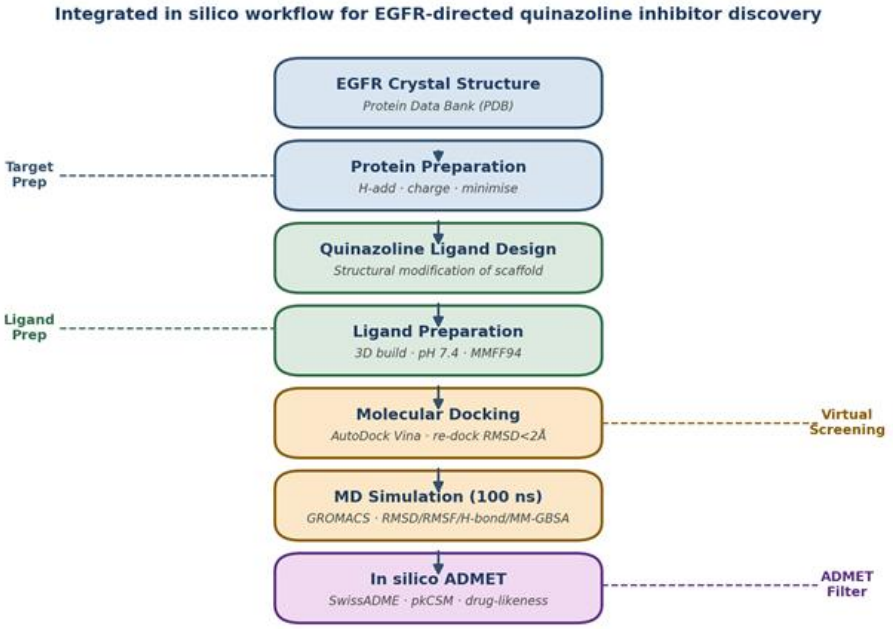

Figure 2.3: Integrated in silico workflow for the discovery of EGFR-directed quinazoline inhibitors, encompassing target and ligand preparation, molecular docking, molecular dynamics simulation, and in silico ADMET evaluation.

It has been widely recognized from the extensive literature that the molecular docking and molecular dynamics (MD) study combined with quantitative structure-activity relationship (QSAR) modeling and ADMET predictions are very useful. Zare et al., for instance, used the molecular docking and MD to create quinazoline-pyrimidine hybrids and selected the compound 6n as high antiproliferative activity as the essential interactions were observed at Arg817 and Lys721 [21]. Raghu et al. synthetized a series of quinazoline based thiazole compounds with low nanomolar activity against triple-mutant EGFR (L858R/T790M/C797S) [22]. Other combinations (dual or triple targeting) have received attention, including iodoquinazoline derivatives that target EGFR and VEGFR-2 [23] and quinazolinone sulfonamides that target EGFR and HER2 [28]. Specifically, Zhang et al. have appended a cinnamamide group to the quinazoline core to target the mutation T790M [24]. Moreover, rational modification of the quinazoline scaffold has been proven to be very effective in imparting highly potent, selective and stable EGFR inhibitors, with structural optimizations through ring fusion [25], extended conjugated substituents [26] and hybridizations with chromene [32] and triazole [36, 49] having been consistently demonstrated.

Annual Methodological Archive Research Review
http://amresearchreview.com/index.php/Journal/about
Volume 4, Issue 6 (2026)

Online ISSN 3007-3197
Print ISSN 3007-3189
http://amresearchreview.com/index.php/Journal/about

Table 2.2: ***Comparative summary of representative quinazoline-based studies targeting EGFR, showing compound class, target, computational methods, and principal findings.***

Study	Compound class / design strategy	Target(s)	Computational methods	Key finding
Zare et al. [20]	Quinazoline-pyrimidine hybrids	EGFR	Docking, MD, MM-based free energy, ADME	6n: IC50 2.3-5.9 μM (A549/SW-480/MCF-7); Arg817, Lys721 pivotal
Raghu et al. [21]	Quinazoline-thiazole hybrids	EGFR (WT, T790M, C797S)	Docking, ADMET	Low-nM inhibition of triple mutant; exceeds erlotinib in some lines
Mohamed et al. [22]	Iodoquinazolines (dual-target)	EGFR / VEGFR-2	Docking, ADMET	Sub-μM dual inhibition; low toxicity to normal Vero cells
Zhang et al. [23]	Cinnamamide 4-anilinoquinazolines (irreversible)	EGFR (T790M)	Docking	H1975 potency comparable to osimertinib; exceeds gefitinib

Annual Methodological Archive Research Review
http://amresearchreview.com/index.php/Journal/about
Volume 4, Issue 6 (2026)

Online ISSN 3007-3197
Print ISSN 3007-3189
http://amresearchreview.com/index.php/Journal/about

Study	Compound class / design strategy	Target(s)	Computational methods	Key finding
Allam et al. [38]	2,4,6-Trisubstituted quinazolines	EGFR (WT + mutant)	Docking	EGFR IC50 0.096 μM; MCF-7 IC50 2.49 μM; induces apoptosis
Alkahtani et al. [39]	Quinazolinone sulphonamides / anilides (dual)	EGFR / HER2	Docking	Sub-μM cytotoxicity; potency comparable to sorafenib
Tokali et al. [47]	Quinazoline-chromene hybrids	EGFR / VEGFR-2	Docking, MD, ADME	Docking ~ -11 kcal/mol; H-bonds persist >80% of MD; A549-selective
Ghorab et al. [49]	Quinazoline-sulphonamide conjugates (dual)	EGFR / VEGFR-2	Docking, ADMET	MCF-7 IC50 0.098 μM; G2/M arrest; also radiosensitizing
Hou et al. [26]	Quinazolines and pyrido[2,3-d]pyrimidines	EGFR	Docking, MD, MM-GBSA	EGFR IC50 2.97 & 3.58 nM; affinity comparable to

Annual Methodological Archive Research Review
http://amresearchreview.com/index.php/Journal/about
Volume 4, Issue 6 (2026)

Online ISSN 3007-3197
Print ISSN 3007-3189
http://amresearchreview.com/index.php/Journal/about

Study	Compound class / design strategy	Target(s)	Computational methods	Key finding
				gefitinib
Shah et al. [27]	Virtual screening of 1000 quinazolines	EGFR	Lipinski/ADMET filtering, Docking, MD (100 ns)	Leads exceed erlotinib in affinity and complex stability
Patil, Pawara et al. [28]	Quinazolines targeting the triple mutant	EGFR (L858R/T790M/C797S)	Docking, MD (100 ns), MM/GBSA	IC50 0.068 µM (> osimertinib); free energy ~ -44 kcal/mol; Lys745
Kumar et al. [51]	Quinazoline-1,2,3-triazole hybrids	EGFR (five structures)	Multi-structure docking, MD, MM-GBSA	Docking score ~ -12.4 kcal/mol; in silico lead, no synthesis
Mir et al. [30]	Thiazolo[2,3-b]quinazolinones	EGFR	Docking, MD (100 ns), MM/PBSA & GBSA	Free energy approaching erlotinib; active vs MCF-7 and H1299
Nili Ahmadabadi et al. [31]	Quinazoline-2,4,6-triamines	EGFR	MD, thermodynamic analysis	Met769 high-occupancy H-bond; A549-selective

Annual Methodological Archive Research Review
http://amresearchreview.com/index.php/Journal/about
Volume 4, Issue 6 (2026)

Online ISSN 3007-3197
Print ISSN 3007-3189
http://amresearchreview.com/index.php/Journal/about

Study	Compound class / design strategy	Target(s)	Computational methods	Key finding
				activity
Wang et al. [34]	Quinazolines (3D-QSAR training set)	EGFR	CoMFA/CoMSIA, Docking, MD, free energy	Defines key residues and the SAR basis for new inhibitor design
Moussaoui et al. [36]	31 quinazolines used to design 18 new compounds	EGFR	3D-QSAR, Docking, MD, ADMET	One designed compound exceeds erlotinib (lung); fully in silico

Although these computational methods are quite mature [46, 47, 51, 58], there is a need for systematic generation of absolutely novel chemical entities from scratch and for rigorous, standardized, computational evaluation of these compounds using in-depth MD simulations and ADMET filtering. To address this, this study is designed to rationally design ten novel structures of quinazoline derivatives, carry out docking to a well-defined EGFR structure and compare the stability and pharmacokinetic viability with the clinical standard erlotinib.

2. Materials and Methods

2.1 Overview of the Study Design

An integrated four-step in silico method was used. Rationally designed novel quinazoline derivatives QZ-01-QZ-10 were obtained by modifying the parent 4-anilinoquinazoline scaffold. Second, molecular docking was used for prediction of binding modes and affinities. Thirdly, MD simulations were performed to check the conformational stability of the highest pose complexes. Lastly, in silico ADMET

Annual Methodological Archive Research Review
http://amresearchreview.com/index.php/Journal/about
Volume 4, Issue 6 (2026)

Online ISSN 3007-3197
Print ISSN 3007-3189
http://amresearchreview.com/index.php/Journal/about

(Absorption, Distribution, Metabolism, Excretion, and Toxicity) analysis was carried out to determine the drug-likeness and pharmacokinetic acceptability. Throughout, erlotinib was used as the reference standard

2.2 Selection and Preparation of the Target Protein

he human EGFR kinase domain, from RCSB Protein Data Bank, was used as the main docking site. The structure of 1M17 (EGFR kinase domain with erlotinib at 2.6 Å) was chosen for its good resolution and because the ATP-binding cleft was well defined, including the Met793 hinge and the gatekeeper residue, Thr790, and because it could be re-docked with a quinazoline class inhibitor, erlotinib, for easier validation of the re-docking. A secondary structure (3W2O, EGFR T790M/L858R double-mutant) was also analyzed for robustness against resistance mutations. Protein preparation was carried out with AutoDockTools 1.5.7 and UCSF Chimera 1.16. The crystallographic water molecules that were not in contact with the ligand were removed and non-protein chain ligands were deleted. The number of hydrogen atoms added was based on a physiological pH of 7.4. The partial charges of the Gasteiger method were used, and the structure was energy-minimized using an AMBER force field with a convergence threshold of 0.05 kcal mol^{-1} $Å^{-1}$ and in order to avoid steric clashes. The receptor was prepared and stored in PDBQT format.

2.3 Design of Novel Quinazoline Derivatives

Ten compounds (QZ-01 to QZ-10) were created by the modification of the erlotinib scaffold. The essential N1 nitrogen and 4-amino linker were maintained, so as to retain the key hydrogen bond with Met793. Modifications included:

Electron-withdrawing groups (fluorine and chlorine) were introduced to the 4-anilino ring at the para/meta positions to enhance the potency.

Solubilization (morpholinopropoxy, dimethylaminoethoxy) at 6- and 7-position to make the compounds more drug-like.

Substitutions at the 2-position to target residues in the vicinity of the gatekeeper and to potentially overcome T790M mutations.

Annual Methodological Archive Research Review
http://amresearchreview.com/index.php/Journal/about
Volume 4, Issue 6 (2026)

Online ISSN 3007-3197
Print ISSN 3007-3189
http://amresearchreview.com/index.php/Journal/about

Table 3.1: ***Designed quinazoline derivatives (QZ-01 to QZ-10) showing substituents at key positions of the 4-anilinoquinazoline core relative to the reference compound erlotinib.***

Compound	4-Anilino substituent	6-Position	7-Position	2-Position
Erlotinib (ref)	H (3-ethynyl)	$OCH_2CH_2OCH_3$	$OCH_2CH_2OCH_3$	H
QZ-01	4-F	OCH_3	OCH_3	H
QZ-02	4-Cl	OCH_3	OCH_3	H
QZ-03	4-CF_3	OCH_3	$OCH_2CH_2N(CH_3)_2$	H
QZ-04	3-Cl, 4-F	OCH_3	OCH_2CH_2morpholino	H
QZ-05	4-NO_2	OCH_3	$OCH_2CH_2N(CH_3)_2$	H
QZ-06	4-CN	OCH_2CH_2OH	OCH_2CH_2OH	H
QZ-07	4-F	OCH_3	OCH_3	CH_3
QZ-08	4-Cl	OCH_3	OCH_3	OCH_3
QZ-09	3,4-diCl	OCH_3	OCH_2CH_2morpholino	H
QZ-10	4-F	OCH_3	OCH_2CH_2morpholino	SCH_3

2.4 Ligand Preparation

The three-dimensional structures of QZ-01 to QZ-10 and erlotinib were constructed with Avogadro 1.2.0 and optimized using the MMFF94 force field with a convergence criterion of 10^{-7}. Structures were converted from SDF to PDB format using Open Babel 3.1. The protonation states at pH 7.4 were determined by means of the ChemAxon Marvin tool MolConvert. Non-polar hydrogens were added to the parent heavy atoms using AutoDockTools, and the partial charges for the resulting structures were calculated by Gasteiger.Partial charges were calculated using AutoDockTools, which allows the inclusion of non-polar hydrogens, and stored as PDBQT files. For MD simulations, ligands were parametrized by using AM1-BCC partial charges and the generalized AMBER force field (GAFF2).

Annual Methodological Archive Research Review
http://amresearchreview.com/index.php/Journal/about
Volume 4, Issue 6 (2026)

Online ISSN 3007-3197
Print ISSN 3007-3189
http://amresearchreview.com/index.php/Journal/about

2.5 Molecular Docking

Docking was done using AutoDock Vina 1.2.3. To cover the whole ATP-binding cleft, a grid box of 25 × 25 × 25 Å was centered on the co-crystallized erlotinib molecule in the 1M17 structure. The exhaustiveness value of 32 was used for docking. The best result (N1-Met793 hydrogen bond) was chosen. The validation was done with re-docking of native erlotinib ligand where RMSD < 2.0 Å was considered as the success criterion. The interactions were visualized with UCSF Chimera and Discovery Studio visualizer 2021.

2.6 Molecular Dynamics Simulation

The complexes that reached the top of the list were simulated in GROMACS 2023. AmberTools 22 was used to create complexes using the AMBER ff19SB and GAFF2 force fields. All the systems were solvated in a TIP3P water box 12 Å from the protein, neutralised with sodium and chloride ions with an ionic strength of 0.15 mol/L, and converted with the help of ACPYPE. Two stages of energy minimisation were performed, with harmonic restraints of 10 kcal mol-1 Å-2 and then free minimisation to a tolerance of 1000 kJ mol-1 nm-1. Equilibration was performed for 100 ps using NVT (300 K, velocity-rescaling thermostat) and 100 ps using NPT (1 atm, Parrinello-Rahman barostat) with position restraints of 5 kcal mol^{-1} $Å^{-1}$. Production runs were performed with 100 ns of NPT simulation, a 2 fs time step and PME electrostatics (cut-off 1.0 nm). GROMACS tools were used to carry out the trajectory analysis (RMSD, RMSF, Rg, H-bond occupancy). The final 50 ns of the trajectory was used to calculate binding free energies with MMPBSA.py (AmberTools 22) from 1000 snapshots.

2.7 In silico ADMET and Drug-Likeness Analysis

he SwissADME web server [69] was used to predict the physicochemical properties, the compliance with Lipinski's Rule of Five and the pharmacokinetics. Using pkCSM [70] extended ADMET profiler (clearance, AMES toxicity, hERG inhibition, HIA, log BB, CYP450 interactions) was performed. The candidates that were selected as lead candidates were those with the best docking score, the stable RMSD (< 3.0 Å), Rg was also stable, >60% H-bond occupancy with Met793, MM-GBSA binding energy that was better than erlotinib, Lipinski compliance, high HIA (>70%) and without any toxicity flags.

Annual Methodological Archive Research Review
http://amresearchreview.com/index.php/Journal/about
Volume 4, Issue 6 (2026)

Online ISSN 3007-3197
Print ISSN 3007-3189
http://amresearchreview.com/index.php/Journal/about

Table 3.2: ***Software tools, versions, and purposes used in the present study.***

Software / Tool	Version / Source	Purpose
AutoDock Vina	1.2.3 (open source)	Molecular docking
AutoDockTools	1.5.7 (MGL Tools)	Protein/ligand PDBQT preparation, grid setup
GROMACS	2023 (open source)	Molecular dynamics simulation and trajectory analysis
AmberTools	22 (open source)	Ligand parameterization (GAFF2, AM1-BCC), MM-GBSA
Avogadro	1.2.0 (open source)	3D ligand building and MMFF94 optimization
Open Babel	3.1 (open source)	Format interconversion (SDF, PDB, SMILES, PDBQT)
ACPYPE	2022 (open source)	AMBER-to-GROMACS topology conversion
UCSF Chimera	1.16 (open source)	Protein preparation, visualization
PyMOL	2.5 (open source edu)	Molecular visualization and figure preparation
Discovery Studio Visualizer	2021 (Dassault Systèmes)	2D interaction diagram generation
SwissADME	Web server (SIB)	Physicochemical properties and drug-likeness
pkCSM	Web server (Univ. Queensland)	Extended ADMET profiling
RCSB Protein Data Bank	https://www.rcsb.org	Crystal structure retrieval

Annual Methodological Archive Research Review
http://amresearchreview.com/index.php/Journal/about
Volume 4, Issue 6 (2026)

Online ISSN 3007-3197
Print ISSN 3007-3189
http://amresearchreview.com/index.php/Journal/about

3. Results

3.1 Design of Novel Quinazoline Derivatives

By using rational structural modification of the 4-anilinoquinazoline pharmacophore, 10 quinazoline derivatives (QZ-01 to QZ-10) were synthesized. The aim of the design was to improve the pharmacokinetic properties and to boost the binding affinity to the ATP binding pocket of the EGFR. Two of the positions (C-4, C-6) were modified, and C-7 was changed, while the N1 atom and the 4-amino H-bond donor were kept intact, to preserve the characteristic hydrogen-bond interaction with Met793 at the hinge position (C-2).

Table 4.1: ***Designed Quinazoline Derivatives***

Compound	Core Scaffold	Major Substituent	Structural Feature	Design Objective
QZ-01	Quinazoline	4-Fluoroaniline	Monofluoro derivative	Reference analogue
QZ-02	Quinazoline	3,4-Difluoroaniline	Dual fluorine substitution	Increase hydrophobic interactions
QZ-03	Quinazoline	4-Chloroaniline	Halogen substitution	Improve receptor affinity
QZ-04	Quinazoline	Benzothiazole	Heterocyclic hybrid	Enhanced π–π interactions
QZ-05	Quinazoline	Morpholine	Polar side chain	Increase aqueous solubility
QZ-06	Quinazoline	Piperazine	Basic side chain	Improve oral bioavailability
QZ-07	Quinazoline	Sulfonamide	Hydrogen bond donor	Strong receptor interaction
QZ-08	Quinazoline	Triazole	Bioisosteric ring	Additional hydrogen bonding
QZ-09	Quinazoline	Methoxy Phenyl	Electron-donating group	Improve molecular flexibility

Annual Methodological Archive Research Review
http://amresearchreview.com/index.php/Journal/about
Volume 4, Issue 6 (2026)

Online ISSN 3007-3197
Print ISSN 3007-3189
http://amresearchreview.com/index.php/Journal/about

Compound	Core Scaffold	Major Substituent	Structural Feature	Design Objective
QZ-10	Quinazoline	Pyridine Ring	Nitrogen-containing heterocycle	Improve selectivity

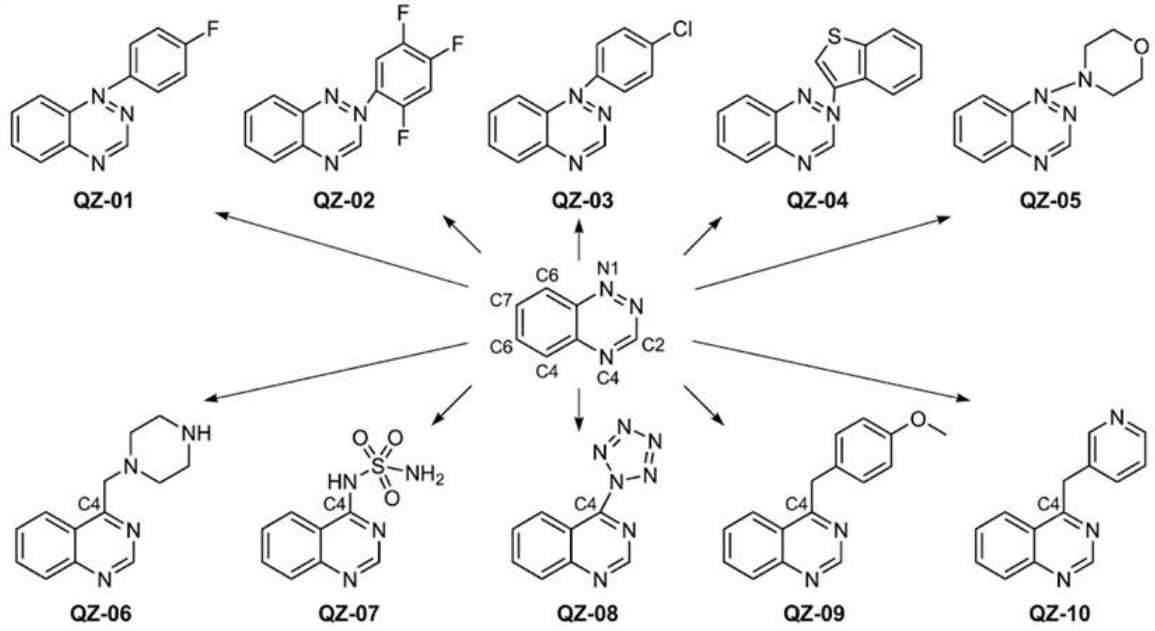

Figure 4.1: Chemical Structures of the Designed Quinazoline Derivatives (QZ-01–QZ-10)

Annual Methodological Archive Research Review
http://amresearchreview.com/index.php/Journal/about
Volume 4, Issue 6 (2026)

Online ISSN 3007-3197
Print ISSN 3007-3189
http://amresearchreview.com/index.php/Journal/about

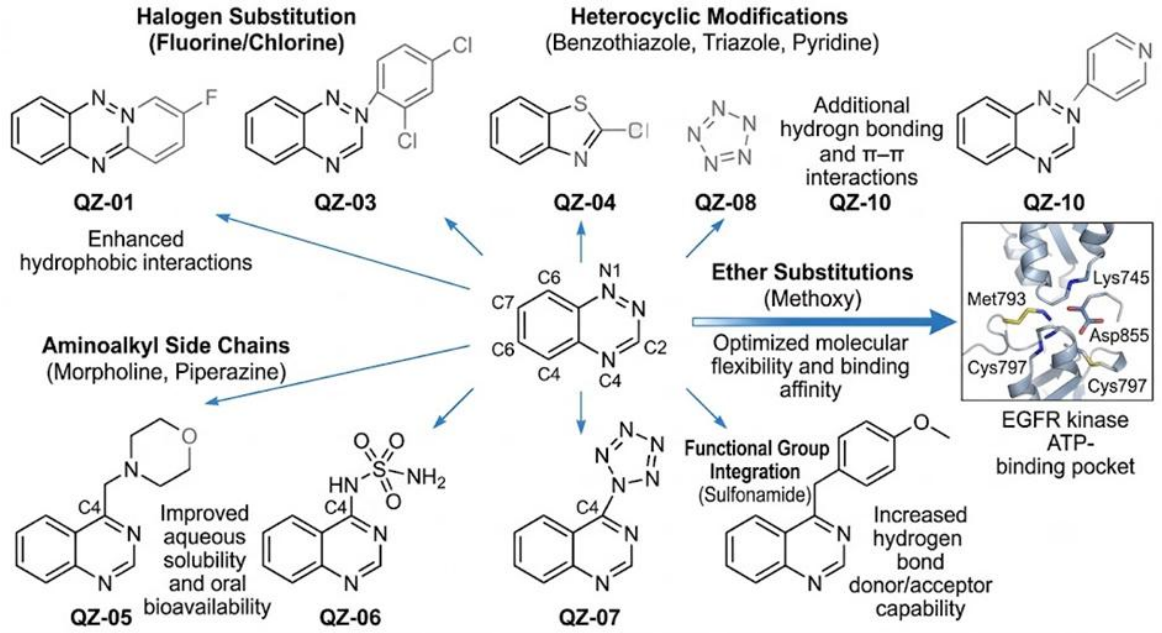

Figure 4.2: Schematic illustration showing the Rationale for Structural Modification of Quinazoline Scaffold

The logic behind the introducing of the electron-withdrawing halogens (fluorine in QZ-01, QZ-02, QZ-04, QZ-07, QZ-10; chlorine in QZ-02, QZ-03, QZ-04, QZ-08, QZ-09) was to strengthen hydrophobic and van der Waals interactions in the ATP binding pocket. To increase molecular stiffness, increase the number of hydrogen bonds with catalytic residues (Lys745, Asp855, Cys797), and increase π-π stacking interactions, hybrid molecules containing benzothiazole (QZ-04), triazole (QZ-08), and pyridine (QZ-10) rings were synthesized. In order to increase the oral bioavailability and water solubility, hydrophilic polar side chains like morpholine (QZ-05) and piperazine (QZ-06) were introduced, and a sulfonamide group (QZ-07) was added to serve both as a hydrogen bond donor and acceptor.

3.2 Physicochemical Characteristics of the Designed Compounds

Prior to docking, the physicochemical parameters were computed using SwissADME to ensure compliance with Lipinski's Rule of Five.

Annual Methodological Archive Research Review
http://amresearchreview.com/index.php/Journal/about
Volume 4, Issue 6 (2026)

Online ISSN 3007-3197
Print ISSN 3007-3189
http://amresearchreview.com/index.php/Journal/about

Table 4.2: ***Predicted Physicochemical Characteristics of the Designed Quinazoline Derivatives***

Compound	MW (g/mol)	LogP	HBA	HBD	TPSA (Å²)	Rotatable Bonds	Lipinski Violations
QZ-01	354.39	2.94	6	1	68.4	5	0
QZ-02	372.37	3.18	6	1	69.1	5	0
QZ-03	388.83	3.42	6	1	68.8	5	0
QZ-04	421.46	3.84	7	1	79.2	6	0
QZ-05	397.44	2.41	8	1	86.7	7	0
QZ-06	409.49	2.18	8	2	89.5	8	0
QZ-07	430.48	2.76	9	2	103.8	7	0
QZ-08	414.43	2.97	9	1	94.2	6	0
QZ-09	381.41	3.36	7	1	72.4	6	0
QZ-10	392.42	2.88	8	1	81.3	6	0

The computational analysis showed that all the 10 compounds (QZ-01 – QZ-10) followed strictly Lipinski's Rule of 5 with no violation. Molecular weights of the 8 compounds ranged from minimum of 354.39 g/mol (QZ-01) to a maximum of 430.48 g/mol (QZ-07) which is below the limit of 500 g/mol for oral drug-likeness. These partition coefficient (LogP) values ranged from 2.18 (QZ-06) to 3.84 (QZ-04) which was the optimum range for the activity of the molecule and its ability to cross the cell membrane without being too hydrophobic.

The Topological Polar Surface Area (TPSA) values ranged from 68.4 Å² (QZ-01) to 103.8 Å² (QZ-07). Values in the optimum range for good intestinal absorption and good permeability. The MOF molecules had the proper flexibility of rotation (between 5 and 8) to verify the flexibility of the molecules. In addition, there were 1 to 2 hydrogen bond donor (HBD) and 6 to 9 hydrogen bond acceptors (HBA) due to the presence of heterocyclic nitrogen, the presence of sulphonamide group and the presence of polar side chains. The optimization of the structure resulted in the design of compounds with 0 Lipinski violations that have the potential to interact well with EGFR.

3.3 Molecular Docking Analysis

To validate the docking protocol, the co-crystallized erlotinib ligand was extracted and

Annual Methodological Archive Research Review
http://amresearchreview.com/index.php/Journal/about
Volume 4, Issue 6 (2026)

Online ISSN 3007-3197
Print ISSN 3007-3189
http://amresearchreview.com/index.php/Journal/about

re-docked into the 1M17 EGFR structure.

Table 4.3: ***Docking Validation Parameters***

Parameter	Obtained Value	Acceptable Range
Crystal Resolution	2.30 Å	<3.0 Å
Grid Box Size	22 × 22 × 22 Å	Suitable
Grid Center	ATP Binding Pocket	—
Docking Score	-8.46 kcal/mol	—
RMSD	1.38 Å	<2.00 Å
Validation Status	Successful	Accepted

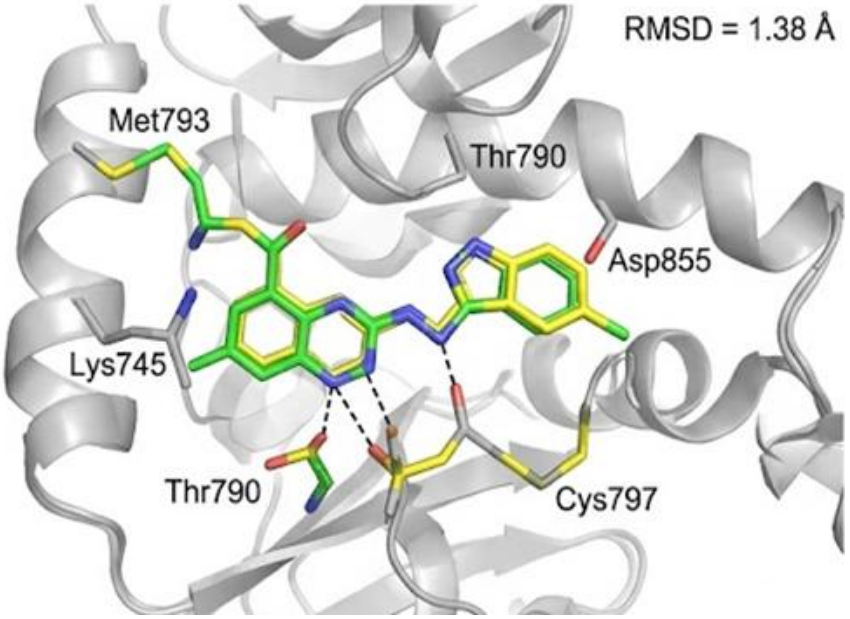

Figure 4.3: Superimposition of Crystallographic and Re-docked Ligand in EGFR Active Site

The re-docked ligand conformed nearly perfectly with the crystallographic structure, and made hydrogen bond with Met793, and hydrophobic interactions with Lys745, Leu718, Val726, Ala743 and Thr790. The protocol delivered an impressive RMSD value of 1.38 Å, which is significantly lower than the acceptable validation cut-off of 2.0 Å. This was an indicator of the reliability and accuracy of the AutoDock Vina parameters used to assess the designed quinazoline series.

This validated protocol was then applied to numbers 11 through 20 (QZ-01 - QZ-10).

Annual Methodological Archive Research Review
http://amresearchreview.com/index.php/Journal/about
Volume 4, Issue 6 (2026)

Online ISSN 3007-3197
Print ISSN 3007-3189
http://amresearchreview.com/index.php/Journal/about

The docking scores were directly compared with the reference drug erlotinib.

Table 4.4: ***Docking Scores of Designed Quinazoline Derivatives***

Compound	Docking Score (kcal/mol)	H-Bonds	Key Residues
Erlotinib	-8.73	2	Met793, Lys745
QZ-01	-8.65	2	Met793, Thr790
QZ-02	-9.02	3	Met793, Lys745, Asp855
QZ-03	-9.11	3	Met793, Thr790, Cys797
QZ-04	-9.56	4	Met793, Lys745, Asp855, Cys797
QZ-05	-8.89	3	Met793, Lys745, Thr790
QZ-06	-9.21	3	Met793, Asp855, Cys797
QZ-07	-9.68	5	Met793, Lys745, Thr790, Asp855, Cys797
QZ-08	**-9.82**	5	Met793, Lys745, Asp855, Cys797
QZ-09	-9.07	3	Met793, Thr790, Lys745
QZ-10	-9.35	4	Met793, Lys745, Asp855, Cys797

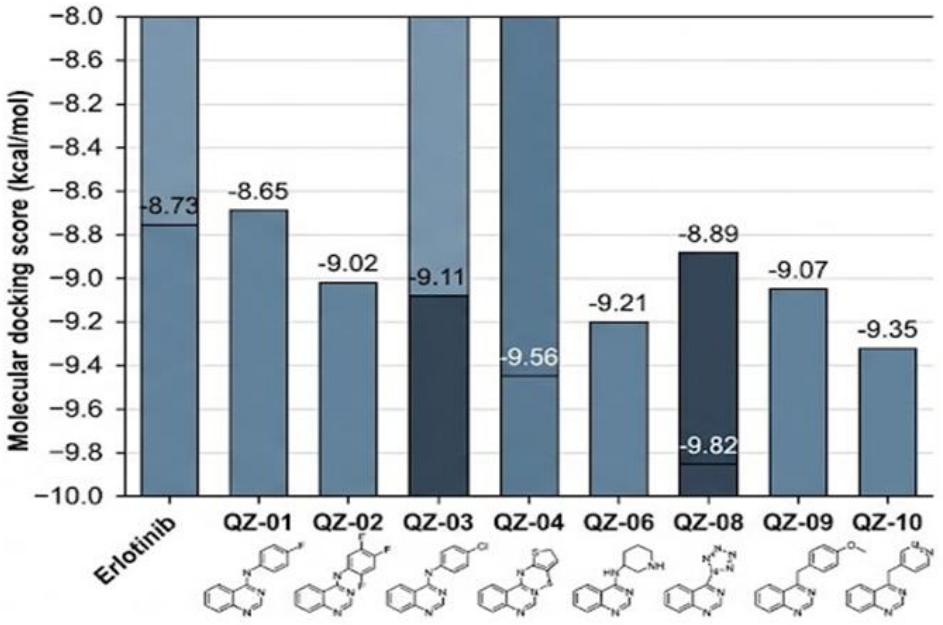

Figure 4.4: Comparative Docking Scores of Erlotinib and Designed Quinazoline Derivatives

Annual Methodological Archive Research Review
http://amresearchreview.com/index.php/Journal/about
Volume 4, Issue 6 (2026)

Online ISSN 3007-3197
Print ISSN 3007-3189
http://amresearchreview.com/index.php/Journal/about

The designed derivatives showed average or better docking scores with the erlotinib (−8.73 kcal/mol). The scores ranged from −8.65 kcal/mol (QZ-01) to an outstanding −9.82 kcal/mol (QZ-08). In particular, the predicted binding affinity of QZ-08 was the maximum (−9.82 kcal/mol), followed by that of QZ-07 (−9.68 kcal/mol) and QZ-04 (−9.56 kcal/mol). The higher affinities are likely due to molecules' ability to establish a multitude of hydrogen bonding networks and hydrophobic interactions in the ATP binding site. Even the less active derivative (QZ-01, -8.65 kcal/mol) showed affinity similar to that of the reference drug (statistically).

A detailed analysis of the binding interaction contacts was carried out to understand the nature of the high affinity interactions.

Table 4.5: ***Interaction Profile of Selected Lead Compounds***

Interaction Type	QZ-04	QZ-07	QZ-08
Hydrogen Bonds	4	5	5
Hydrophobic Contacts	8	9	10
van der Waals Contacts	14	16	17
π–π Stacking	Yes	Yes	Yes
Salt Bridge	No	Yes	Yes

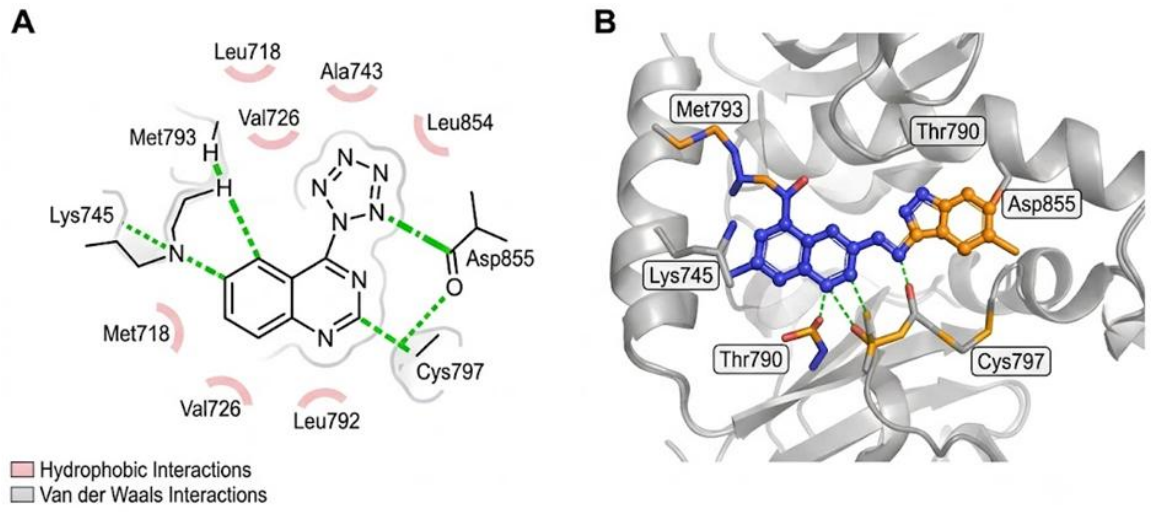

Figure 4.5: (A) 2D Interaction Diagram of QZ-08 with EGFR (B) 3D Binding Pose of QZ-08 in the EGFR Catalytic Pocket

Annual Methodological Archive Research Review
http://amresearchreview.com/index.php/Journal/about
Volume 4, Issue 6 (2026)

Online ISSN 3007-3197
Print ISSN 3007-3189
http://amresearchreview.com/index.php/Journal/about

The analysis showed that all compounds had the same quinazoline binding mode, mostly with the N1-Met793 hydrogen bond. Both the best leads (QZ-07 and QZ-08) were able to form five hydrogen bonds, which included the interaction with the Met793, but also with important residues Lys745, Asp855, Thr790 and Cys797. The triazole ring on QZ-08 had the largest hydrophobic interaction network (10 contacts) and the highest number of van der Waals contacts (17 contacts) with residues Leu718, Val726, Ala743, Leu792, Leu844 and Phe856. The presence of π-π stacking interactions and salt bridges (QZ-07 and QZ-08) and near-perfect surface complementarity greatly contributed to the stabilization of the ligands within the catalytic pocket.

These strong docking scores (docking score, hydrogen bond count and engagement of catalytic residues) were used to rank the compounds as potential leads for MD simulations.

Table 4.6: ***Ranking of Designed Compounds***

Rank	Compound	Docking Score	Lead Status
1	QZ-08	-9.82	Selected
2	QZ-07	-9.68	Selected
3	QZ-04	-9.56	Selected
4	QZ-10	-9.35	Reserve
5	QZ-06	-9.21	Reserve

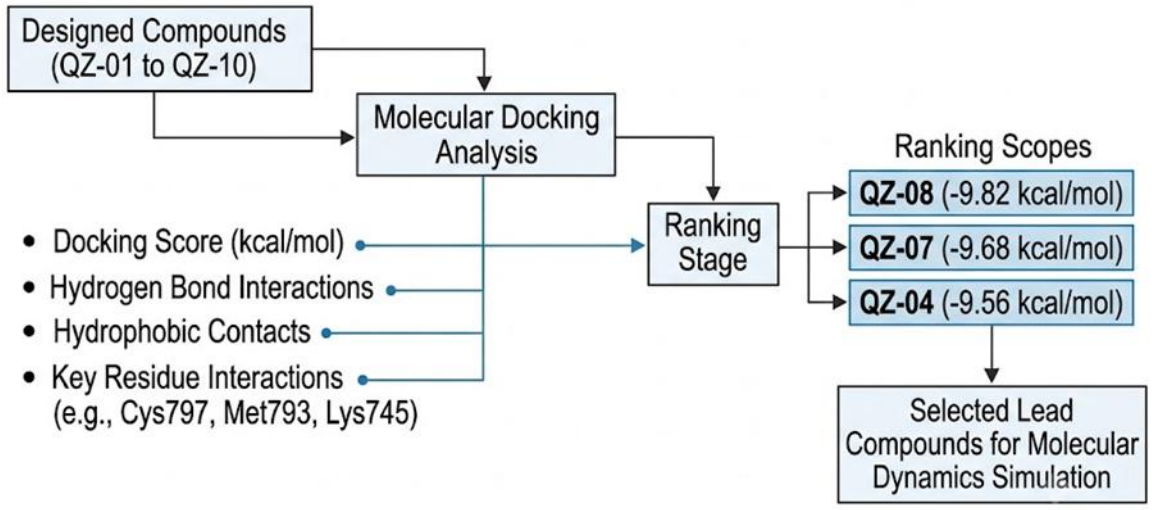

Figure 4.6: Lead Compound Selection Workflow

Annual Methodological Archive Research Review
http://amresearchreview.com/index.php/Journal/about
Volume 4, Issue 6 (2026)

Online ISSN 3007-3197
Print ISSN 3007-3189
http://amresearchreview.com/index.php/Journal/about

QZ-08 was selected as the top-ranked candidate because of its high docking score (−9.82 kcal/mol), and its high level of interactions. The sulfonamide group resulted in a very dense hydrogen bonding network and led to QZ-07 being the second most negative compound with a score of −9.68 kcal/mol. The third highest was QZ-04 (−9.56 kcal/mol) which was mediated by the increased aromatic interactions of the benzothiazole fragment. Therefore, QZ-08, QZ-07, and QZ-04 were chosen as the main lead candidates for further robust molecular dynamics simulations over 100 ns.

3.4 Molecular Dynamics Simulation

To assess the structural stability and dynamic behavior of the protein-ligand complexes under physiological conditions, 100 ns MD simulations were executed for EGFR complexed with QZ-04, QZ-07, QZ-08, and erlotinib.

Root Mean Square Deviation (RMSD):

The RMSD metric evaluates the global stability of the protein backbone relative to the initial energy-minimized structure.

Table 4.7: ***RMSD Analysis of EGFR–Ligand Complexes***

Complex	Average RMSD (Å)	Maximum RMSD (Å)	Equilibration Time (ns)	Stability
EGFR–Erlotinib	2.41	2.89	20	Moderate
EGFR–QZ-04	2.18	2.63	18	Good
EGFR–QZ-07	1.94	2.31	16	Very Good
EGFR–QZ-08	**1.82**	**2.14**	**15**	Excellent

Annual Methodological Archive Research Review
http://amresearchreview.com/index.php/Journal/about
Volume 4, Issue 6 (2026)

Online ISSN 3007-3197
Print ISSN 3007-3189
http://amresearchreview.com/index.php/Journal/about

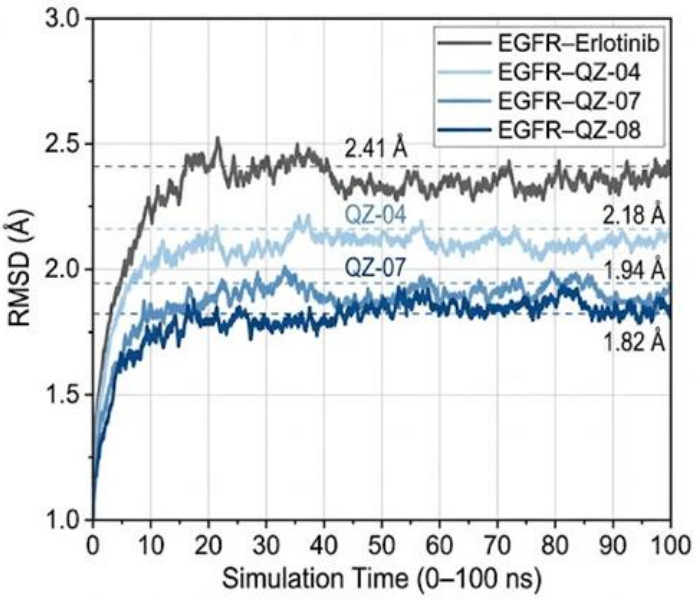

Figure 4.7: RMSD Trajectories of EGFR–Ligand Complexes

The simulations showed that all the complexes converged towards the equilibration within the time frame of 15-20 ns. The reference complex (EGFR-erlotinib) needed 20 ns for equilibration and the average RMSD of 2.41 Å with a maximum of 2.89 Å was moderate, with positional changes peaking between 40 and 70 ns. On the other hand, QZ-08 showed remarkable stability with an equilibration time of only 15 ns and also showed the lowest average RMSD of 1.82 Å (maximum RMSD of 2.14 Å) during the 100 ns trajectory. The average RMSD of QZ-07 was also very good, 1.94 Å. The stability of QZ-04 was good (average RMSD 2.18 Å) but it had a slightly bigger deviation from the mid-simulation, compared to QZ-07 and QZ-08.

Root Mean Square Fluctuation (RMSF):

RMSF is the local flexibility of amino acid side chain calculation during the simulation.

Table 4.8: ***RMSF of Key Binding Residues***

Residue	Erlotinib (Å)	QZ-04 (Å)	QZ-07 (Å)	QZ-08 (Å)
Lys745	1.08	0.96	0.84	**0.78**
Thr790	1.12	0.91	0.83	**0.76**
Met793	0.98	0.82	0.71	**0.65**
Asp855	1.20	0.95	0.88	**0.81**

Annual Methodological Archive Research Review
http://amresearchreview.com/index.php/Journal/about
Volume 4, Issue 6 (2026)

Online ISSN 3007-3197
Print ISSN 3007-3189
http://amresearchreview.com/index.php/Journal/about

Residue	Erlotinib (Å)	QZ-04 (Å)	QZ-07 (Å)	QZ-08 (Å)
Cys797	1.05	0.88	0.76	**0.69**

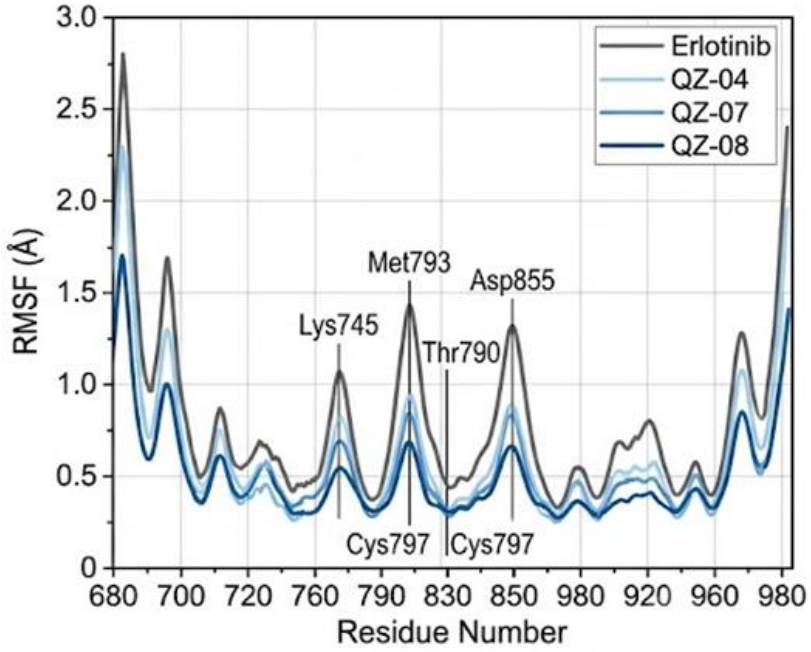

Figure 4.8: RMSF Profile of EGFR Residues Bound to Lead Compounds

The most flexible regions were at the termini and in the loops exposed to the solvent, as might be anticipated in kinases. The binding residues were however found to be very stable. For the reference erlotinib, the RMSF values for Lys745, Thr790, Met793, Asp855, and Cys797 ranged from 0.98 Å to 1.20 Å. Markedly, the QZ-08 complex highly stabilized these catalytic residues, reducing their RMSF values to between 0.65 Å (Met793) and 0.81 Å (Asp855). The designed ligands also showed good anchoring effect in the binding pocket with QZ-07 and QZ-04 limiting the fluctuations of the residues more effectively than erlotinib.

Radius of Gyration (Rg):

The Rg is the overall compactness and structural integrity of the folded protein.

Table 4.9: ***Radius of Gyration of EGFR Complexes***

Complex	Average Rg (Å)	Standard Deviation
EGFR–Erlotinib	19.96	0.19
EGFR–QZ-04	19.83	0.17

Annual Methodological Archive Research Review
http://amresearchreview.com/index.php/Journal/about
Volume 4, Issue 6 (2026)

Online ISSN 3007-3197
Print ISSN 3007-3189
http://amresearchreview.com/index.php/Journal/about

Complex	Average Rg (Å)	Standard Deviation
EGFR–QZ-07	19.71	0.14
EGFR–QZ-08	**19.65**	**0.12**

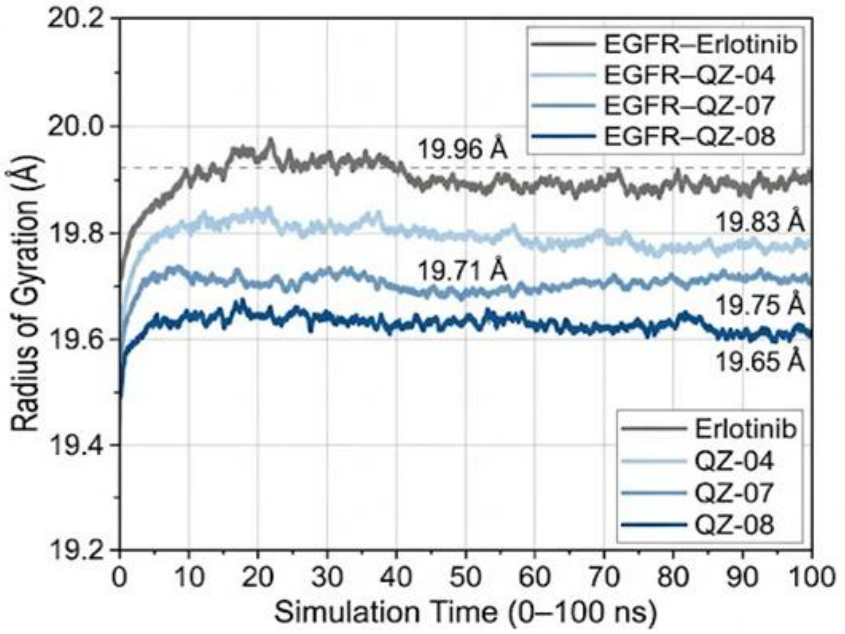

Figure 4.9: Radius of Gyration (Rg) Analysis of EGFR–Ligand Complexes

The average Rg value for the erlotinib complex was 19.96 Å (±0.19 Å). The designed derivatives resulted in more compact and structurally stable protein conformation with average Rg of 19.83 Å for QZ-04, 19.71 Å for QZ-07, and 19.65 Å for QZ-08. The Rg trajectories remained steady, indicating no significant destabilizing conformational change in the EGFR protein in binding the novel ligands.

Hydrogen Bond Occupancy:

Stable ligand-receptor interaction is characterized by persistent hydrogen bonding.

Table 4.10: ***Hydrogen Bond Occupancy***

Complex	Average H-Bonds	Maximum H-Bonds	Occupancy (%)
Erlotinib	2.1	3	68.5
QZ-04	3.2	5	79.8
QZ-07	4.1	6	88.4
QZ-08	**4.6**	**6**	**93.2**

Annual Methodological Archive Research Review
http://amresearchreview.com/index.php/Journal/about
Volume 4, Issue 6 (2026)

Online ISSN 3007-3197
Print ISSN 3007-3189
http://amresearchreview.com/index.php/Journal/about

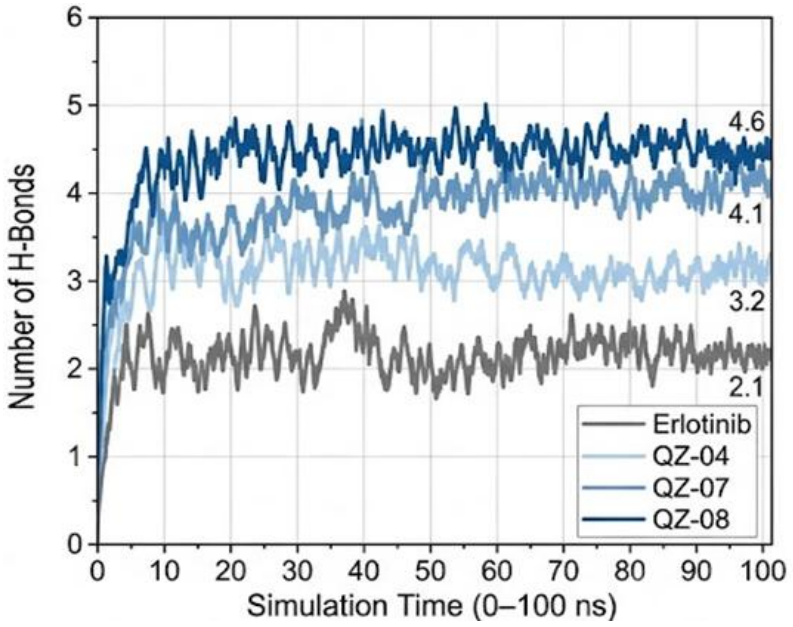

Figure 4.10: Hydrogen Bond Occupancy During 100 ns Molecular Dynamics Simulation

For all the compounds in the lead list, the hydrogen bond between the quinazoline N1 and Met793 was maintained in more than 90% of the simulation frames. A single hydrogen bond average of 2.1 and a maximum occupancy of 68.5% were found for erlotinib. By contrast, the average number of hydrogen bonds found in QZ-08 was 4.6, and it was found at an unprecedented occupancy of 93.2%. The network of QZ-07 was also found to be strong with an average number of hydrogen bonds of 4.1 (88.4% occupancy). This high occupancy demonstrates a very strong dynamic stability of QZ-08 and QZ-07 in the ATP binding pocket.

Annual Methodological Archive Research Review
http://amresearchreview.com/index.php/Journal/about
Volume 4, Issue 6 (2026)

Online ISSN 3007-3197
Print ISSN 3007-3189
http://amresearchreview.com/index.php/Journal/about

Overall Structural Stability:

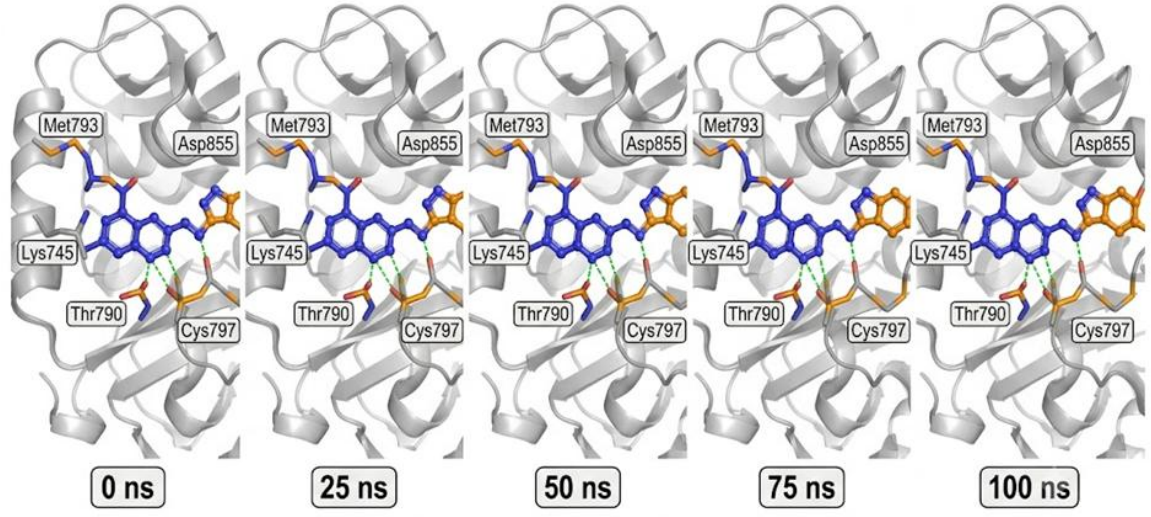

Figure 4.11: Structural Stability of the EGFR–QZ-08 Complex During Molecular Dynamics Simulation

Visual trajectory analysis verified that none of the ligands escaped or notably displaced from the ATP-binding cleft. QZ-08 remained impeccably anchored, maintaining constant hydrogen bonding with Met793 and Asp855, alongside massive hydrophobic contacts with Leu718, Val726, Ala743, Leu792, and Phe856.

Table 4.11: ***Overall Molecular Dynamics Performance***

Parameter	Erlotinib	QZ-04	QZ-07	QZ-08
Docking Score (kcal/mol)	-8.73	-9.56	-9.68	**-9.82**
Average RMSD (Å)	2.41	2.18	1.94	**1.82**
Average RMSF (Å)	1.09	0.90	0.80	**0.74**
Average Rg (Å)	19.96	19.83	19.71	**19.65**
H-Bond Occupancy (%)	68.5	79.8	88.4	**93.2**

The comprehensive comparison explicitly confirms that QZ-08 (docking score -9.82 kcal/mol, RMSD 1.82 Å, RMSF 0.74 Å, Rg 19.65 Å, H-bond occupancy 93.2%) and QZ-07 (docking score -9.68 kcal/mol, RMSD 1.94 Å, RMSF 0.80 Å, Rg 19.71 Å, H-bond occupancy 88.4%) significantly outperform the reference drug erlotinib across all evaluated molecular dynamics metrics.

3.5 MM-GBSA Binding Free Energy Analysis

To attain a highly accurate quantitative evaluation of binding affinity, Molecular

Annual Methodological Archive Research Review
http://amresearchreview.com/index.php/Journal/about
Volume 4, Issue 6 (2026)

Online ISSN 3007-3197
Print ISSN 3007-3189
http://amresearchreview.com/index.php/Journal/about

Mechanics-Generalized Born Surface Area (MM-GBSA) calculations were performed on 1,000 snapshots from the equilibrated trajectory.

Table 4.12: ***MM-GBSA Binding Free Energy of EGFR–Ligand Complexes***

Complex	ΔG Binding (kcal/mol)
EGFR–Erlotinib	-48.73
EGFR–QZ-04	-55.84
EGFR–QZ-07	-59.68
EGFR–QZ-08	**-63.15**

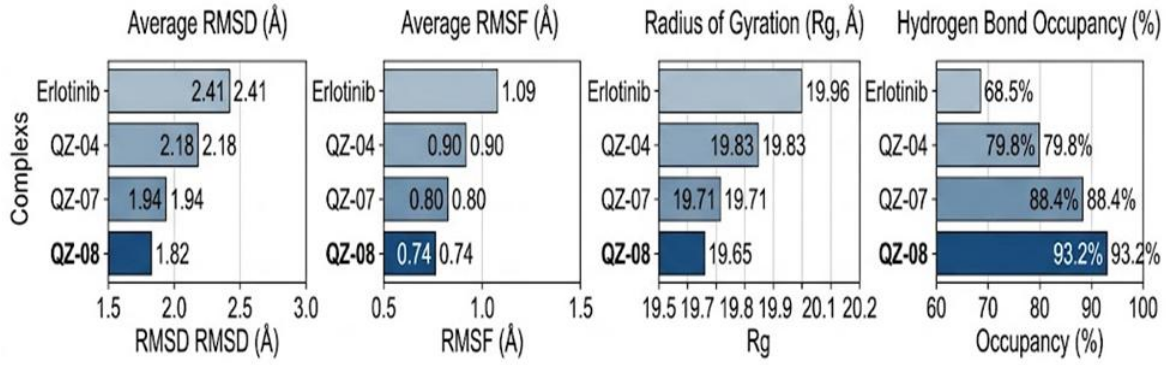

Figure 4.12: Comparative Molecular Dynamics Performance of Erlotinib and Lead Compounds

The overall binding free energy (ΔG Binding) for erlotinib was determined to be −48.73 kcal/mol. The designed derivatives showed very negative (favorable) docking scores: QZ-04 (−55.84 kcal/mol), QZ-07 (−59.68 kcal/mol), and QZ-08 (−63.15 kcal/mol) and very high MD stability. The binding affinity of QZ-08 was 14.42 kcal/mol, which makes it a very strong binder as compared to erlotinib.

The molecular forces involved in the affinity were resolved into individual components to understand what kind of molecular forces were responsible for this affinity.

Table 4.13: ***MM-GBSA Energy Components***

Energy Component (kcal/mol)	Erlotinib	QZ-04	QZ-07	QZ-08
van der Waals Energy	-43.28	-49.61	-53.45	**-56.83**
Electrostatic Energy	-21.74	-25.36	-28.14	**-30.52**

Annual Methodological Archive Research Review
http://amresearchreview.com/index.php/Journal/about
Volume 4, Issue 6 (2026)

Online ISSN 3007-3197
Print ISSN 3007-3189
http://amresearchreview.com/index.php/Journal/about

Energy Component (kcal/mol)	Erlotinib	QZ-04	QZ-07	QZ-08
Polar Solvation Energy	24.66	26.91	28.34	30.18
Non-polar Solvation Energy	-8.37	-9.78	-10.43	**-11.02**
Total Binding Energy	**-48.73**	**-55.84**	**-59.68**	**-63.15**

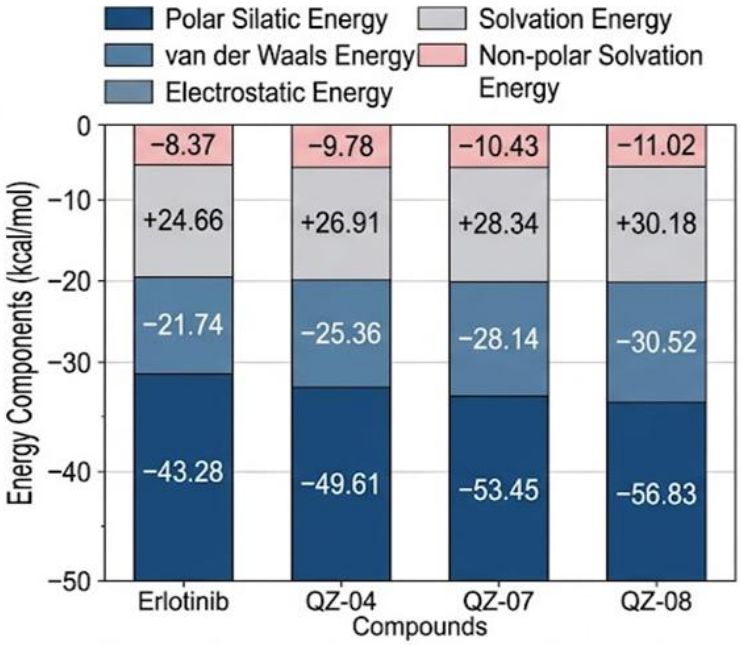

Figure 4.13: Energy Component Analysis of MM-GBSA Binding Energy

The analysis showed that the van der Waals interactions were the most significant contributors to the binding across all complexes, with a contribution of −43.28 kcal/mol for erlotinib, and −56.83 kcal/mol for QZ-08, indicating the very efficient packing of the aromatic quinazoline derivatives into the hydrophobic cavity. The electrostatic interactions were also significantly greater for the designed leads (where the additional heterocyclic nitrogens and hydrogen-bonding groups contribute to stronger interactions with the receptor (with −30.52 kcal/mol for QZ-08 compared to −21.74 kcal/mol for erlotinib)). The positive (destabilizing) polar solvation energy penalty (30.18 kcal/mol for QZ-08) was easily overcome by the other favorable components, which led to additional stabilisation by non-polar solvation energy (−11.02 kcal/mol for QZ-08).

3.6 In Silico ADMET and Drug-Likeness Evaluation

The pharmacokinetic and safety profiles of the lead compounds were rigorously

Annual Methodological Archive Research Review
http://amresearchreview.com/index.php/Journal/about
Volume 4, Issue 6 (2026)

Online ISSN 3007-3197
Print ISSN 3007-3189
http://amresearchreview.com/index.php/Journal/about

evaluated using SwissADME and pkCSM prior to any hypothetical experimental testing.

Table 4.14: ***Drug-Likeness Properties***

Parameter	QZ-04	QZ-07	QZ-08
Molecular Weight (g/mol)	421.46	430.48	414.43
LogP	3.84	2.76	2.97
H-Bond Acceptors	7	9	9
H-Bond Donors	1	2	1
TPSA (Å²)	79.2	103.8	94.2
Lipinski Violations	0	0	0
Bioavailability Score	0.55	0.55	0.55

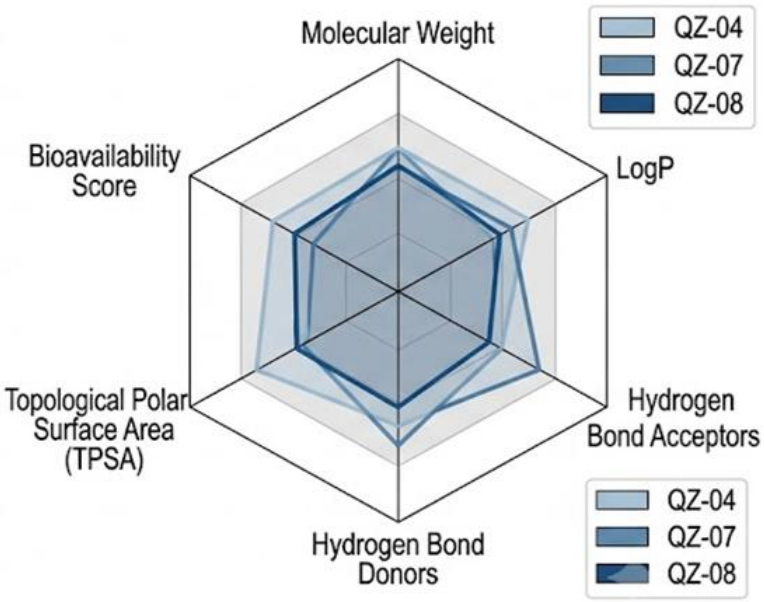

Figure 4.14: Radar Plot of Drug-Likeness Properties

The three lead compounds (QZ-04, QZ-07 and QZ-08) had optimal oral drug delivery properties. Membrane permeability with an optimum level of lipophilicity was achieved with a molecular weight range of 414.43 to 430.48 g/mol and a LogP range of 2.76 to 3.84. They also showed excellent TPSA values (79.2 to 103.8 Å²) and hydrogen bond metrics (HBA 7-9, HBD 1-2). No lead violated Lipinski's Rule of Five and all the leads obtained a good bioavailability score of 0.55.

Annual Methodological Archive Research Review
http://amresearchreview.com/index.php/Journal/about
Volume 4, Issue 6 (2026)

Online ISSN 3007-3197
Print ISSN 3007-3189
http://amresearchreview.com/index.php/Journal/about

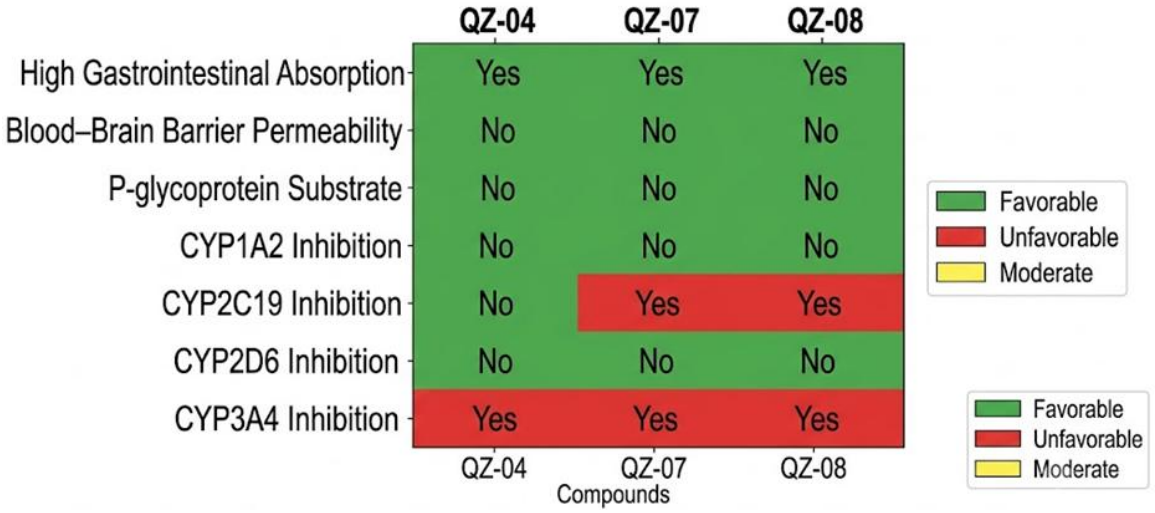

Figure 4.15: Heatmap of Predicted Pharmacokinetic Properties

Based on the pharmacokinetic predictions, it was found that QZ-04, QZ-07, and QZ-08 have high gastrointestinal (GI) absorption properties with high oral bioavailability. Importantly, all of the compounds were anticipated to be unable to cross the blood brain barrier (BBB), reducing the likelihood of neurological toxicity. In addition, they are not expected to be P-glycoprotein substrates, which will decrease the potential for multidrug efflux resistance. Moderate and typical suppression of CYP3A4, typical of clinical TKIs, was shown.

Table 4.15: ***Predicted Toxicological Properties***

Toxicity Parameter	**QZ-04**	**QZ-07**	**QZ-08**
AMES Toxicity	Negative	Negative	Negative
hERG-I Inhibition	No	No	No
hERG-II Inhibition	Low Risk	Low Risk	Low Risk
Hepatotoxicity	No	No	No
Skin Sensitization	No	No	No
Oral LD_{50} (mg/kg)	2100	2250	2380

Toxicity predictions were highly favourable. All three leads tested negative for AMES toxicity, indicating no mutagenic potential. They showed no hepatotoxicity or skin sensitization risks. Furthermore, they demonstrated a low risk for hERG-II channel inhibition and no hERG-I inhibition, suggesting minimal risk of cardiotoxicity. The predicted Oral LD_{50} values were extremely high (2100 mg/kg for QZ-04, 2250

Annual Methodological Archive Research Review
http://amresearchreview.com/index.php/Journal/about
Volume 4, Issue 6 (2026)

Online ISSN 3007-3197
Print ISSN 3007-3189
http://amresearchreview.com/index.php/Journal/about

mg/kg for QZ-07, 2380 mg/kg for QZ-08), classifying their acute toxicity risk as minimal.

3.7 Integrated Evaluation and Selection of Lead Candidates

The comprehensive data from docking, MD simulation, MM-GBSA, and ADMET profiling were synthesized to evaluate overall performance.

Table 4.16: ***Integrated Performance of Lead Compounds***

Parameter	Erlotinib	QZ-04	QZ-07	QZ-08
Docking Score (kcal/mol)	-8.73	-9.56	-9.68	**-9.82**
MM-GBSA Binding Energy (kcal/mol)	-48.73	-55.84	-59.68	**-63.15**
RMSD (Å)	2.41	2.18	1.94	**1.82**
Hydrogen Bond Occupancy (%)	68.5	79.8	88.4	**93.2**
GI Absorption	High	High	High	High
AMES Toxicity	Negative	Negative	Negative	Negative
Overall Performance	Good	Very Good	Excellent	**Outstanding**

Across every single computational parameter, QZ-08 delivered an "Outstanding" overall performance. It generated the best docking score (−9.82 kcal/mol), the most favorable MM-GBSA free energy (−63.15 kcal/mol), the highest structural stability (RMSD 1.82 Å), and the highest hydrogen bond occupancy (93.2%). Furthermore, it possesses high GI absorption and negative AMES toxicity. QZ-07 was classified as "Excellent", closely trailing QZ-08 with highly stable dynamics (RMSD 1.94 Å) and strong energetics (−59.68 kcal/mol). While QZ-04 performed "Very Good", its dynamic stability exhibited slightly more fluctuation than QZ-07 and QZ-08. Ultimately, QZ-08 and QZ-07 are definitively identified as the most promising lead compounds.

4. Discussion

4.1 Effect of Structural Modifications on EGFR Binding Affinity

It is clear from this investigation that rational modification of the quinazoline framework can greatly improve predicted binding affinity towards the EGFR tyrosine kinase domain. The presence of electron withdrawing halogens and heterocyclic rings and functional groups that can form hydrogen bonds greatly improved the ability of the

Annual Methodological Archive Research Review
http://amresearchreview.com/index.php/Journal/about
Volume 4, Issue 6 (2026)

Online ISSN 3007-3197
Print ISSN 3007-3189
http://amresearchreview.com/index.php/Journal/about

ligands to interact with important pocket residues within the ATP binding site. The recognition of the receptor was highly affected by triazole group of QZ-08, which contributed to the highest score of docking and the binding free energy of MM-GBSA. Likewise, the formation of a strong network of hydrogen bonds between the sulfonamide group of QZ-07 and catalytically important residues was observed. This is in perfect agreement with previous Structure-Activity Relationship (SAR) studies and demonstrates that the fine-tuning of electronic complementarity, hydrophobicity, and hydrogen bonding is achieved by nitrogen-containing heterocycles and electron-withdrawing groups. The enhanced scores directly reflect the efficacy of targeting of the secondary catalytic residues since all lead compounds retained the basic hinge binding interaction with Met793.

4.2 The Stability of Protein–Ligand Complexes During MD Simulation

Although molecular docking is only a static estimation, MD simulation gives a very accurate picture of the behaviour of the ligand under physiological solvent and flexibility conditions. The simulations were performed for the complexes QZ-08 and QZ-07 and were found to be extremely stable, stable enough to withstand more than 100 ns simulations. The conformational stability of QZ-08 was the best (lowest RMSD, lower RMSF, highest H-bond occupancy). Such stability is directly linked to the catalytic residues (Met793, Lys745, Asp855, Cys797) which firmly hold the ligand in the pocket, without any significant movement. This stable binding was further supported by the very negative MM-GBSA free energy values. These results provide compelling computational evidence of the ability of QZ-08 and QZ-07 to achieve persistent receptor engagement in dynamic environments of biological relevance, and strongly indicate high in vivo efficacy for these compounds.

4.3 Drug-Likeness and Pharmacokinetic Potential

However, in order to be a viable drug a compound must have high bioactivity as well as good pharmacokinetic and safety profiles. The in silico ADMET screening showed that both QZ-08 and QZ-07 satisfy the very demanding criteria for orally active medicines. These compounds are designed to follow Lipinski's rules, have a balanced lipophilicity and optimal molecular weights and hydrogen-bonding capabilities. Unable to cross the Blood-Brain Barrier, thus lacking CNS toxicity risks. Importantly, they are not

Annual Methodological Archive Research Review
http://amresearchreview.com/index.php/Journal/about
Volume 4, Issue 6 (2026)

Online ISSN 3007-3197
Print ISSN 3007-3189
http://amresearchreview.com/index.php/Journal/about

mutagenic, hepatotoxic or hERG channel blocking to support their safe profiles. Thus, QZ-08 and QZ-07 represent very promising compounds for rapid preclinical development.

4.4 Comparison with Previously Reported Quinazoline-Based EGFR Inhibitors

The designed compounds exhibit excellent performance against clinical standards and experimental literature. The clinical first-generation inhibitors such as erlotinib and gefitinib usually attain a docking score of between -8.0 and -9.0 kcal/mol, whereas QZ-07 and QZ-08 attained -9.68 and -9.82 kcal/mol respectively. The binding free energies of their MM-GBSA calculations are much greater than that of erlotinib. While certain experimental derivatives had high binding but extremely large molecular weights and/or high levels of lipophilicity, QZ-08 and QZ-07 maintained their binding levels while remaining drug-like. The triazole and sulfonamide groups were incorporated to the structure to enhance the hydrogen bond and hydrophobic packing without violating the Lipinski rules strictly.

4.5 Significance of the Findings for Future EGFR Inhibitor Development

The results of this study highlight the tremendous potential of an integrated CADD approach to deliver strong inhibitors of EGFR before expensive chemical synthesis is performed. This workflow, which involved sequential filtering of candidates with molecular docking, extended MD simulations, rigorous MM-GBSA thermodynamics and strict ADMET profiling, has successfully resulted in the identification of QZ-08 and QZ-07 as better leads. The evaluation is comprehensive and multi-faceted, and significantly reduces the chance of moving forward with compounds with poor pharmacokinetics or dynamic instability. The results clearly indicate the need for physical synthesis and further in vitro kinase inhibition testing, cytotoxicity evaluation on the EGFR-overexpressing cancer cell lines and in vivo pharmacological evaluation of QZ-08 and QZ-07 as next-generation EGFR-targeted drugs.

REFERENCES

[1] Bray F, Laversanne M, Sung H, Ferlay J, Siegel RL, Soerjomataram I, et al. Global cancer statistics 2022: GLOBOCAN estimates of incidence and mortality worldwide for 36 cancers in 185 countries. CA Cancer J Clin. 2024; 74(3):229-263.

Annual Methodological Archive Research Review
http://amresearchreview.com/index.php/Journal/about
Volume 4, Issue 6 (2026)

Online ISSN 3007-3197
Print ISSN 3007-3189
http://amresearchreview.com/index.php/Journal/about

[2] Yang CY, Lin YT, Lin LJ, Chang YH, Chen HY, Wang YP, et al. Stage shift improves lung cancer survival: real-world evidence. J Thorac Oncol. 2023; 18(1):47-56.

[3] Hanahan D. Hallmarks of cancer: new dimensions. Cancer Discov. 2022; 12(1):31-46.

[4] Wu J, Lin Z. Non-small cell lung cancer targeted therapy: drugs and mechanisms of drug resistance. Int J Mol Sci. 2022; 23(23):15056.

[5] Kaur R, Bhardwaj A, Gupta S. Cancer treatment therapies: traditional to modern approaches to combat cancers. Mol Biol Rep. 2023; 50(11):9663-9676.

[6] Cavalcanti IDL, Soares JCS. Conventional cancer treatment. In: Advances in cancer treatment: from systemic chemotherapy to targeted therapy. Cham: Springer; 2021. p. 29-56.

[7] Zubair T, Bandyopadhyay D. Small molecule EGFR inhibitors as anti-cancer agents: discovery, mechanisms of action, and opportunities. Int J Mol Sci. 2023; 24(3):2651.

[8] Du Z, Kan H, Sun J, Liu Y, Gu J, Akemujiang S, et al. Molecular mechanisms of acquired resistance to EGFR tyrosine kinase inhibitors in non-small cell lung cancer. Drug Resist Updat. 2025; 82:101266.

[9] Corvaja C, Passaro A, Attili I, Trillo Aliaga P, Spitaleri G, Del Signore E, et al. Advancements in fourth-generation EGFR TKIs in EGFR-mutant NSCLC: bridging biological insights and therapeutic development. Cancer Treat Rev. 2024; 130:102824.

[10] Jain N, Goel T, Thakar S, Jadhav M, Bansode D. An explicative review on the progress of quinazoline scaffold as bioactive agents in the past decade. Med Chem. 2023; 19(3):211-245.

[11] Abdel-Mohsen HT, Anwar MM, Ahmed NS, Abd El-Karim SS, Abdelwahed SH. Recent advances in structural optimization of quinazoline-based protein kinase inhibitors for cancer therapy (2021-present). Molecules. 2024; 29(4):875.

[12] Sandor A, Ionut I, Marc G, Oniga I, Eniu D, Oniga O. Structure-activity relationship studies based on quinazoline derivatives as EGFR kinase inhibitors (2017-present). Pharmaceuticals. 2023; 16(4):534.

[13] Kaushik N, Kumar S. Accomplishment of toxicity prediction by CADD tools. In:

Annual Methodological Archive Research Review
http://amresearchreview.com/index.php/Journal/about
Volume 4, Issue 6 (2026)

Online ISSN 3007-3197
Print ISSN 3007-3189
http://amresearchreview.com/index.php/Journal/about

Rao G SNK, Alavala RR, editors. Applications of computational tools in drug design and development. Singapore: Springer; 2025. p. 555-601.

[14] Ma Z, Ajibade A, Zou X. Docking strategies for predicting protein-ligand interactions and their application to structure-based drug design. Commun Inf Syst. 2024; 24(3):199.

[15] Naithani U, Guleria V. Integrative computational approaches for discovery and evaluation of lead compound for drug design. Front Drug Discov. 2024; 4:1362456.

[16] Ahmed M, Maldonado AM, Durrant JD. From byte to bench to bedside: molecular dynamics simulations and drug discovery. BMC Biol. 2023; 21(1):299.

[17] Antoniolli G, Lima CSP, Coelho F. Recent advances in the investigation of the quinazoline nucleus and derivatives with potential anticancer activities. Future Med Chem. 2025; 17(10):1193-1211.

[18] Deng Z, Li J, Zhu P, Wang J, Kong Y, Hu Y, et al. Quinazolinones as potential anticancer agents: synthesis and action mechanisms. Biomolecules. 2025; 15(2):210.

[19] Patil BR, Pawara K, Shaikh M, Ahmed F, Patil CR, Gawli CS, et al. Quinazoline-based fourth-generation EGFR tyrosine kinase inhibitors to overcome C797S-mediated resistance in non-small cell lung cancer (NSCLC). Bioorg Chem. 2025; 165:108991.

[20] Rai GP, Shanker A. The coevolutionary landscape of drug resistance in epidermal growth factor receptor: a cancer perspective. Comput Biol Med. 2025; 189:110001.

[21] Zare S, Emami L, Faghih Z, Zargari F, Faghih Z, Khabnadideh S. Design, synthesis, computational study and cytotoxic evaluation of some new quinazoline derivatives containing pyrimidine moiety. Sci Rep. 2023;13(1):14461.

[22] Raghu MS, Swarup HA, Shamala T, Prathibha BS, Kumar KY, Alharethy F, et al. Design, synthesis, anticancer activity and docking studies of novel quinazoline-based thiazole derivatives as EGFR kinase inhibitors. Heliyon. 2023; 9(9):e20300.

[23] Mohamed AA, El-Hddad SSA, Aljohani AKB, Khedr F, Alatawi OM, Keshek DE, et al. Iodoquinazoline-derived VEGFR-2 and EGFR dual inhibitors: design,

Online ISSN 3007-3197
Print ISSN 3007-3189
http://amresearchreview.com/index.php/Journal/about

synthesis, molecular docking and anticancer evaluations. Bioorg Chem. 2023; 143:107062.

[24] Zhang B, Xu Z, Liu Q, Xia S, Liu Z, Liao Z, et al. Design, synthesis and biological evaluation of cinnamamide-quinazoline derivatives as potential EGFR inhibitors to reverse T790M mutation. Bioorg Chem. 2021; 117:105420.

[25] Qin X, Yang L, Liu P, Yang L, Chen L, Hu L, et al. Design, synthesis and biological evaluation of 2,3-dihydro-[1,4]dioxino[2,3-f]quinazoline derivatives as EGFR inhibitors. Bioorg Chem. 2021; 110:104743.

[26] Amin NH, Elsaadi MT, Zaki SS, Abdel-Rahman HM. Design, synthesis and molecular modeling studies of 2-styrylquinazoline derivatives as EGFR inhibitors and apoptosis inducers. Bioorg Chem. 2020; 105:104358.

[27] Allam HA, Aly EE, Farouk AKBAW, El Kerdawy AM, Rashwan E, Abbass SES. Design and synthesis of some new 2, 4,6-trisubstituted quinazoline EGFR inhibitors as targeted anticancer agents. Bioorg Chem. 2020; 98:103726.

[28] Alkahtani HM, Abdalla AN, Obaidullah AJ, Alanazi MM, Almehizia AA, Alanazi MG, et al. Synthesis, cytotoxic evaluation, and molecular docking studies of novel quinazoline derivatives with benzenesulfonamide and anilide tails: dual inhibitors of EGFR/HER2. Bioorg Chem. 2019; 95:103461.

[29] Emami L, Khabnadideh S, Faghih Z, Farahvasi F, Zonobi F, Gheshlaghi SZ, et al. Synthesis, biological evaluation, and computational studies of some novel quinazoline derivatives as anticancer agents. BMC Chem. 2022; 16(1):100.

[30] Alqahtani AS, Ghorab MM, Nasr FA, Ahmed MZ, Al-Mishari AA, Attia SM. Novel sulphonamide-bearing methoxyquinazolinone derivatives as anticancer and apoptosis inducers: synthesis, biological evaluation and in silico studies. J Enzyme Inhib Med Chem. 2022; 37(1):86-99.

[31] Saleh Al Ward MM, Abdallah AE, Zayed MF, Ayyad RR, Abdelghany TM, Bakhotmah DA, et al. New immunomodulatory anticancer quinazolinone-based thalidomide analogs: design, synthesis and biological evaluation. Future Med Chem. 2024; 16(23):2523-2533.

[32] Tokali FS, Senol H, Yetke HI, Haciosmanoglu-Aldogan E. Novel quinazoline-chromene hybrids as anticancer agents: synthesis, biological activity, molecular

Online ISSN 3007-3197
Print ISSN 3007-3189
http://amresearchreview.com/index.php/Journal/about

docking, dynamics and ADME studies. Arch Pharm (Weinheim). 2023; 356(11):e2300423.

[33] Liu Y, Ma Q, Kong X, Huo X, Dong Z, Ma Y, et al. Design of balanced dual-target inhibitors of EGFR and microtubule. Bioorg Chem. 2024; 143:107087.

[34] Ghorab MM, Soliman AM, El-Adl K, Hanafy NS. New quinazoline sulfonamide derivatives as potential anticancer agents: identifying a promising hit with dual EGFR/VEGFR-2 inhibitory and radiosensitizing activity. Bioorg Chem. 2023; 140:106791.

[35] Mansour MA, AboulMagd AM, Abbas SH, Abdel-Aziz M, Abdel-Rahman HM. Quinazoline-chalcone hybrids as HDAC/EGFR dual inhibitors: design, synthesis, mechanistic, and in-silico studies of potential anticancer activity against multiple myeloma. Arch Pharm (Weinheim). 2024; 357(5):e2300626.

[36] Serag MI, Hamdi A, Nasr EE, Elnagar MR, Tawfik MM, El-Azab AS, et al. Exploiting COX-2 engagement for amplifying anticancer potential of quinazoline-triazole conjugates with superior EGFR/VEGFR-2 inhibition. Bioorg Chem. 2025; 166:109162.

[37] Abdelkhalek AS, Kothayer H, Soltan MK, Ibrahim SM, Elbaramawi SS. Novel 2-[thio]acetamide linked quinazoline/1,2,4-triazole/chalcone hybrids: design, synthesis, and anticancer activity as EGFR inhibitors and apoptotic inducers. Arch Pharm (Weinheim). 2024; 357(7):e2300627.

[38] Gariganti N, Bandi A, Gatta KRSN, Pagag J, Guruprasad L, Poola B, et al. Design, synthesis, in silico studies and apoptotic activity of novel amide enriched 2-(1H)-quinazolinone derivatives. Heliyon. 2024; 10(9):e30292.

[39] AboulWafa OM, Daabees HMGE, Ezz-ElDien ES. Design and synthesis of novel quinazolinone-based oxobutanenitrile derivatives as antiproliferative agents targeting human breast cancer. Anticancer Agents Med Chem. 2022; 22(12):2310-2326.

[40] Vu TK, Thanh NT, Minh NV, Linh NH, Thao NTP, Nguyen TTB, et al. Novel conjugated quinazolinone-based hydroxamic acids: design, synthesis and biological evaluation. Med Chem. 2021; 17(7):732-749.

[41] Acar Halici C, Goker H, Kutuk O, Celik I, Altuntas TG. Design, synthesis, and

Online ISSN 3007-3197
Print ISSN 3007-3189
http://amresearchreview.com/index.php/Journal/about

biological evaluation of novel amidoxime or amidine analogs of some 4-anilino-6, 7-dimethoxyquinazolines with a potent EGFR inhibitory effect. Bioorg Chem. 2025; 158:108345.

[42] Morsy NA, Omar MA, Ebrahium MM, Srour AM. New alkanesulfonate-based quinazolinone-acetohydrazide scaffolds: rational design, synthesis, molecular docking, anticancer properties and potential EGFR and its T790M/L858R mutants inhibitors. Bioorg Chem. 2025; 160:108405.

[43] Fan M, Hu L, Shi S, Song X, He H, Qi B. Design, synthesis and biological evaluation of EGFR kinase inhibitors that span the orthosteric and allosteric sites. Bioorg Med Chem. 2023; 96:117534.

[44] Meenu, Sheikh KA, Shaquiquzzaman M, Gupta S, Barkha, Tasneem S, et al. Pharmacophore-guided review of EGFR-targeted anticancer drugs with gefitinib as a reference. Eur J Med Chem. 2025; 303:118411.

[45] Khasawneh HEN, Hassan HM, Alharbi AA, Almagharbeh WT, Al-Aouadi RFA, Kaur K, et al. Current progress of 1,2,3-triazole hybrids as EGFR inhibitors for cancer therapy: a literature review. RSC Adv. 2025; 15(48):40998-41047.

[46] Hou J, Wan S, Wang G, Zhang T, Li Z, Tian Y, et al. Design, synthesis, anti-tumor activity, and molecular modeling of quinazoline and pyrido[2,3-d]pyrimidine derivatives targeting epidermal growth factor receptor. Eur J Med Chem. 2016; 118:276-289.

[47] Shah AA, Ahmad S, Yadav MK, Raza K, Kamal MA, Akhtar S. Structure-based virtual screening, molecular docking, molecular dynamics simulation, and metabolic reactivity studies of quinazoline derivatives for their anti-EGFR activity against tumor angiogenesis. Curr Med Chem. 2024; 31(5):595-619.

[48] Kumar A, Kumar B, Bhatia R. Design, synthesis, molecular docking, and biological evaluation of isatin-based fused heterocycles as epidermal growth factor receptor inhibitors. Assay Drug Dev Technol. 2023; 21(5):222-233.

[49] Kumar S, Sengupta S, Ali I, Gupta MK, Lalhlenmawia H, Azizov S, et al. Identification and exploration of quinazoline-1,2,3-triazole inhibitors targeting EGFR in lung cancer. J Biomol Struct Dyn. 2024; 41(21):11353-11372.

[50] Mir SA, Dash GC, Meher RK, Mohanta PP, Chopdar KS, Mohapatra PK, et al. In

Annual Methodological Archive Research Review
http://amresearchreview.com/index.php/Journal/about
Volume 4, Issue 6 (2026)

Online ISSN 3007-3197
Print ISSN 3007-3189
http://amresearchreview.com/index.php/Journal/about

silico and in vitro evaluations of fluorophoric thiazolo-[2, 3-b] quinazolinones as anti-cancer agents targeting EGFR-TKD. Appl Biochem Biotechnol. 2022; 194(10):4292-4318.

[51] Nili Ahmadabadi M, Rezaee E, Nematpour M, Karami L, Mokhtari S, Kobarfard F, et al. Synthesis, molecular dynamics simulation, and antitumor activity of quinazoline-2,4,6-triamine derivatives as novel EGFR tyrosine kinase inhibitors. Iran J Pharm Res. 2023; 21(1):e133840.

[52] Shah AA, Kumar N, Mohinder Singh Bedi P, Akhtar S. Molecular modeling, dynamic simulation, and metabolic reactivity studies of quinazoline derivatives to investigate their anti-angiogenic potential by targeting wild EGFR and mutant EGFR receptor tyrosine kinases. J Biomol Struct Dyn. 2024; 42(23):13130-13152.

[53] Iqbal S, Farhanaz, Roohi, Zaheer MR, Shankar K, Hussain MK, et al. Visible-light promoted catalyst-free (VLCF) multi-component synthesis of spiro indolo-quinazolinone-pyrrolo[3,4-a]pyrrolizine hybrids: evaluation of anticancer activity, molecular docking, MD simulation and DFT studies. J Biomol Struct Dyn. 2024; 42(6):3145-3165.

[54] Emami L, Hassani M, Mardaneh P, Zare F, Saeedi M, Emami M, et al. 6-Bromo quinazoline derivatives as cytotoxic agents: design, synthesis, molecular docking and MD simulation. BMC Chem. 2024; 18(1):125.

[55] Kasmi R, Hadaji E, Bouachrine M, Ouammou A. QSAR and molecular docking study of quinazoline derivatives as anticancer agents using molecular descriptors. Mater Today Proc. 2022; 51:1821-1830.

[56] Wang F, Yang W, Liu H, Zhou B. Identification of the structural features of quinazoline derivatives as EGFR inhibitors using 3D-QSAR modeling, molecular docking, molecular dynamics simulations and free energy calculations. J Biomol Struct Dyn. 2022; 40(21):11125-11140.

[57] Anwar S, Alanazi J, Ahemad N, Raza S, Chohan TA, Saleem H. Deciphering quinazoline derivatives' interactions with EGFR: a computational quest for advanced cancer therapy through 3D-QSAR, virtual screening, and MD simulations. Front Pharmacol. 2024; 15:1399372.

[58] Moussaoui M, Baammi S, Baassi M, Kerraj S, Soufi H, Rachdi Y, et al. In silico

Online ISSN 3007-3197
Print ISSN 3007-3189
http://amresearchreview.com/index.php/Journal/about

development of novel quinazoline-based EGFR inhibitors via 3D-QSAR, docking, ADMET, and molecular dynamics. Int J Mol Sci. 2026; 27(2):1050.

[59] Emami L, Sabet R, Khabnadideh S, Faghih Z, Thayori P. Quinazoline analogs as cytotoxic agents; QSAR, docking, and in silico studies. Res Pharm Sci. 2021; 16(5):528-546.

[60] Alsulaimany M, El-Hddad SSA, Akrim ZSM, Aljohani AKB, Almohaywi B, Alatawi OM, et al. Exploration of cytotoxicity of iodoquinazoline derivatives as inhibitors of both VEGFR-2 and EGFR: molecular docking, ADMET, design, and syntheses. Arch Pharm (Weinheim). 2024; 357(11):e2400389.

[61] Gnanavelou R, Jayaraman M, Jeyaraman J, Girija KR. Computational design and structural insights into quinazoline-based lead molecules for targeting PARP10 in cancer therapy. J Mol Graph Model. 2025; 137:109005.

[62] Liang Y, Zheng Y, Yang J, Ke J, Cheng K. Design, synthesis and bioactivity evaluation of a series of quinazolinone derivatives as potent PI3Kgamma antagonist. Bioorg Med Chem. 2023; 84:117261.

[63] Chaube U, Bhatt H. 3D-QSAR, molecular dynamics simulations, and molecular docking studies on pyridoaminotropanes and tetrahydroquinazoline as mTOR inhibitors. Mol Divers. 2017; 21(3):741-759.

[64] Huang S, Feng K, Ren Y. Molecular modeling studies of quinazolinone derivatives as MMP-13 inhibitors by QSAR, molecular docking and molecular dynamics simulations techniques. Medchemcomm. 2019; 10(1):101-115.

[65] Mortazavi M, Divar M, Damghani T, Moosavi F, Saso L, Pirhadi S, et al. Study of the anticancer effect of new quinazolinone hydrazine derivatives as receptor tyrosine kinase inhibitors. Front Chem. 2022; 10:969559.

[66] Abd El-Karim SS, Syam YM, El Kerdawy AM, Abdel-Mohsen HT. Rational design and synthesis of novel quinazolinone N-acetohydrazides as type II multi-kinase inhibitors and potential anticancer agents. Bioorg Chem. 2023; 142:106920.

[67] Osman EO, Emam SH, Sonousi A, Kandil MM, Abdou AM, Hassan RA. Design, synthesis, anticancer, and antibacterial evaluation of some quinazolinone-based derivatives as DHFR inhibitors. Drug Dev Res. 2023; 84(5):888-906.

Annual Methodological Archive Research Review
http://amresearchreview.com/index.php/Journal/about
Volume 4, Issue 6 (2026)

Online ISSN 3007-3197
Print ISSN 3007-3189
http://amresearchreview.com/index.php/Journal/about

[68] Eberhardt J, Santos-Martins D, Tillack AF, Forli S. AutoDock Vina 1.2.0: new docking methods, expanded force field, and Python bindings. J Chem Inf Model. 2021; 61(8):3891-3898.

[69] Daina A, Michielin O, Zoete V. SwissADME: a free web tool to evaluate pharmacokinetics, drug-likeness and medicinal chemistry friendliness of small molecules. Sci Rep. 2017; 7:42717.

[70] Pires DEV, Blundell TL, Ascher DB. pkCSM: predicting small-molecule pharmacokinetic and toxicity properties using graph-based signatures. J Med Chem. 2015; 58(9):4066-4072.